

Survey of charge symmetry breaking operators for $dd \rightarrow \alpha\pi^0$

A. Gårdestig* and C. J. Horowitz

*Department of Physics and Nuclear Theory Center,
Indiana University, Bloomington, IN 47405*

A. Nogga

Institute for Nuclear Theory, University of Washington, Seattle, WA 98195-1550

A. C. Fonseca

Centro Física Nuclear, Universidade de Lisboa, 1649-003 Lisboa, Portugal

C. Hanhart

Institut für Kernphysik, Forschungszentrum Jülich, Jülich, Germany

G. A. Miller

Department of Physics, University of Washington, Seattle, WA 98195-1560

J. A. Niskanen

Department of Physical Sciences, University of Helsinki, Helsinki, Finland

U. van Kolck

*Department of Physics, University of Arizona, Tucson, AZ 85721 and
RIKEN BNL Research Center, Brookhaven National Laboratory, Upton, NY 11973*

(Dated: November 11, 2018)

Abstract

The charge-symmetry-breaking amplitudes for the recently observed $dd \rightarrow \alpha\pi^0$ reaction are investigated. Chiral perturbation theory is used to classify and identify the leading-order terms. Specific forms of the related one- and two-body tree level diagrams are derived. As a first step toward a full calculation, a few tree-level two-body diagrams are evaluated at each considered order, using a simplified set of d and α wave functions and a plane-wave approximation for the initial dd state. The leading-order pion-exchange term is shown to be suppressed in this model because of poor overlap of the initial and final states. The higher-order one-body and short-range (heavy-meson-exchange) amplitudes provide better matching between the initial and final states and therefore contribute significantly and coherently to the cross section. The consequences this might have for a full calculation, with realistic wave functions and a more complete set of amplitudes, are discussed.

PACS numbers: 11.30.Hv, 25.10.+s, 25.45.-z

Keywords: charge symmetry breaking, neutral pion production

*Present address: Department of Physics and Astronomy, Ohio University, Athens, OH 45701; Electronic address: anders@phy.ohiou.edu

I. INTRODUCTION

For most practical purposes, hadronic isospin states can be considered as charge symmetric, i.e., invariant under a rotation by 180° around the 2-axis in isospin space. Charge symmetry CS is thus a subset of the general isospin symmetry, charge independence CI, which requires invariance under *any* rotation in isospin space. In quantum chromodynamics QCD, CS means that the dynamics are unchanged under the exchange of the up and down quarks [1]. In the language of hadrons, this symmetry translates into, e.g., the invariance of the strong interaction under the exchange of protons and neutrons. However, since the up and down quarks do have different masses ($m_u \neq m_d$) [2, 3], the QCD Lagrangian is not charge symmetric and neither is the strong interaction of hadrons. This symmetry violation is called charge symmetry breaking CSB. There is also a contribution to CSB because of the different electromagnetic interactions of the up and down quarks.

Observing the effects of CSB interactions therefore provides a probe of m_u and m_d , which are fundamental, but poorly known, parameters of the standard model. The quantity m_d is larger than m_u , causing a specific pattern of mass splitting between members of an isospin multiplet [1]. In particular, the light quark mass difference causes the neutron to be heavier than the proton. If this were not the case, our universe would be very different, as a consequence of the dependence of Big-Bang nucleosynthesis on the relative abundances of protons and neutrons.

Experimental evidence for CSB has been demonstrated in $\rho^0\omega$ mixing [4], the nucleon mass splitting, the binding-energy difference of mirror nuclei such as ^3H and ^3He [5], the different scattering lengths of elastic nn and pp scattering [6], and in the minute but well-measured difference between the proton and neutron analyzing powers of elastic np scattering [7]. A recent theoretical analysis of πN scattering data found a small CSB effect [8].

Studying the $dd \rightarrow \alpha\pi^0$ reaction presents exciting new opportunities for developing the understanding of CSB. This reaction obviously violates isospin conservation; but more specifically, it violates charge symmetry since the deuterons and the α -particle are self-conjugate under the charge-symmetry operator, with a positive eigenvalue, while the neutral pion wave function changes sign. This reaction could not occur if charge symmetry were conserved, and the cross section is proportional to the square of the CSB amplitude. This is unique because all other observations of CSB involve interferences with charge symmetric amplitudes. Thus

a very clean signal for CSB is obtained through the observation of a non-zero cross section. Furthermore this process has a close connection with QCD because chiral symmetry plays a dominant role in determining pion-production cross sections.

Lapidus, in 1956 [9], was the first to realize that the $dd \rightarrow \alpha\pi^0$ reaction would be a useful probe of CSB. Various experimental groups tried to observe it, but without success [10]. After other attempts yielding only upper limits [11], a group at the Saturne accelerator in Saclay reported a non-vanishing $dd \rightarrow \alpha\pi^0$ cross section at $T_d = 1.1$ GeV [12]. This finding was refuted by members of the same collaboration who argued that the putative signal for π^0 production actually was caused by the $dd \rightarrow \alpha\gamma\gamma$ background [13]. The importance of this background was confirmed by calculations of the double radiative capture [14], using a model based on a very successful treatment of the $dd \rightarrow \alpha\pi\pi$ reaction at similar energies [15]. Thus the Saclay $dd \rightarrow \alpha\pi^0$ cross section is almost certainly a misinterpretation of a heavily-cut smooth $dd \rightarrow \alpha\gamma\gamma$ background [14].

There have been two exciting recent observations of CSB in experiments involving the production of neutral pions. Many years of effort have led to the observation of CSB in $np \rightarrow d\pi^0$ at TRIUMF. After a careful treatment of systematic errors, the CSB forward-backward asymmetry of the differential cross section was found to be $A_{\text{fb}} = [17.2 \pm 8(\text{stat}) \pm 5.5(\text{sys})] \times 10^{-4}$ [16]. In addition, the final experiment at the IUCF Cooler ring has reported a very convincing $dd \rightarrow \alpha\pi^0$ signal near threshold ($\sigma = 12.7 \pm 2.2$ pb at $T_d = 228.5$ MeV and 15.1 ± 3.1 pb at 231.8 MeV), superimposed on a smooth $dd \rightarrow \alpha\gamma\gamma$ background [17]. This background is roughly a factor two larger than calculations based on Ref. [14], but has the expected shape. The data are consistent with the pion being produced in an *s*-wave, as expected from the proximity of the threshold ($T_d = 225.6$ MeV).

Clearly, these new high-quality CSB experiments demand a theoretical interpretation using fundamental CSB mechanisms. At momenta comparable to the pion mass, $Q \sim m_\pi$, QCD and its symmetries (and in particular CSB) can be described by a hadronic effective field theory EFT, chiral perturbation theory χ PT [18, 19]. This EFT has been extended to pion production [20, 21, 22, 23, 24] where typical momenta are $Q \sim \sqrt{m_\pi M}$, with M the nucleon mass. (See also Ref. [25] where pion production was studied neglecting this large momentum in power counting.) This formalism provides specific CSB effects in addition to the nucleon mass difference. In particular, there are two pion-nucleon seagull interactions related by chiral symmetry to the quark-mass and electromagnetic contributions to the

nucleon mass difference [26, 27].

It was demonstrated for the CI reactions $\pi\pi \rightarrow \pi\pi$ [28], $\pi N \rightarrow \pi N$ [18], and $NN \rightarrow NN$ [29] that the values of the low energy constants can be understood as the low energy limit of the exchange of a heavy state. This procedure is called the resonance saturation hypothesis. Within this scheme the other CSB interactions, also caused by the light quark mass difference [26, 30], can be viewed as the low-momentum limit of standard meson-exchange mechanisms, such as π - η - η' and ρ - ω mixing. Determining the various interaction strengths may provide significant information about the quark mass difference. Since these terms contribute to CSB in the reactions $np \rightarrow d\pi^0$ and $dd \rightarrow \alpha\pi^0$ with different weights, it is important to analyze both processes using the same framework.

Early calculations of CSB in $np \rightarrow d\pi^0$ [31, 32] incorporated most of the relevant mechanisms, giving an asymmetry — dominated by π - η mixing — of the order of -2×10^{-3} for energies near threshold [32]. The combined pion-nucleon seagull interactions required by chiral symmetry generate a larger contribution with the opposite sign [33], and provide a prediction for $A_{\text{fb}}(np \rightarrow d\pi^0)$ (based on a crude estimate of the strength of the CSB rescattering contribution) that was confirmed by the recent experimental observation. However, the experimental value is in the lower band of the predicted range of values of A_{fb} .

Our aim here is to provide the first study of CSB in the near threshold $dd \rightarrow \alpha\pi^0$ reaction using chiral EFT techniques. The effect of π - η - η' mixing on this reaction was studied several years ago at $T_d = 1.95$ GeV [34]. Pion production was assumed to be dominated by the production of η and η' , followed by π - η or π - η' mixing. Using phenomenological information on these parameters and on the η - η' angle, the cross section was expressed in terms of existing data for the η production cross sections. This method cannot be used for energies lower than that required to produce an η meson, and other CSB contributions cannot be evaluated this way.

It is necessary to explicitly account for the detailed dynamics of the few-nucleon pion-production amplitudes. Therefore we will discuss the CSB amplitudes in the first few orders, defined according to a chiral counting scheme that provides a general guide to the expected importance of different interaction terms. Such schemes do not explicitly account for spin-isospin factors, for the sometimes poor overlap of wave functions, or for the spin and isospin dependence of the wave functions. We shall see that selection rules resulting from the use of specific wave functions and the threshold kinematics have a strong impact on the relative

importance of particular diagrams.

The fast incoming deuterons ($p \sim 460$ MeV/c in the center-of-momentum frame c.m.) need to be slowed down to produce an α -particle and an s -wave pion at threshold. The resulting large momentum transfer can be transmitted through the initial- and final-state interactions or wave function distortions, and through the exchange of a particle in the pion-production sub-amplitude. Only the latter two possibilities will be considered here. The complexities of the dd initial state interaction will be included in a future study. Thus, we expect that a pion-production sub-amplitude should preferentially provide for momentum sharing between the deuterons, in order to avoid forcing the nucleons out into the small, high-momentum tail of the α -particle wave function.

Spin, isospin, and symmetry requirements restrict the partial waves allowed for the $dd \rightarrow \alpha\pi^0$ reaction. In the spectroscopic notation ${}^{2S+1}L_J l$, where S , L , J are the spin, orbital, and total angular momenta of the dd state and l is the pion angular momentum, the lowest partial waves are ${}^3P_0 s$ and ${}^5D_1 p$. Hence, production of an s -wave pion requires that the initial deuterons be in a relative P -wave, with spins coupled to a spin-1 state, coupled together to zero total angular momentum. The deuteron spins then need to be flipped, while absorbing the P -wave, to form the spin-0 state of the helium nucleus. The invariant amplitude therefore takes the form $\mathbf{p} \cdot (\boldsymbol{\epsilon}_1 \times \boldsymbol{\epsilon}_2)$ where \mathbf{p} is the deuteron relative momentum and $\boldsymbol{\epsilon}_{1,2}$ are the polarization vectors of the initial deuterons. On the other hand, a p -wave pion is produced only when the deuterons are in a relative D -wave, with spins maximally aligned to spin 2, requiring either a coupling with $\Delta L = \Delta S = 2$ or D -states of d or α . This invariant amplitude is of the form $\mathbf{p} \cdot \boldsymbol{\epsilon}_1 \mathbf{p} \cdot (\boldsymbol{\epsilon}_2 \times \mathbf{p}_\pi) + \mathbf{p} \cdot \boldsymbol{\epsilon}_2 \mathbf{p} \cdot (\boldsymbol{\epsilon}_1 \times \mathbf{p}_\pi)$, where \mathbf{p}_π is the pion momentum. Interferences between s and p -waves will disappear for any unpolarized observable.

In addition to these momentum-sharing and overall symmetry considerations, the spin-isospin symmetries of the nucleons in the $dd:\alpha$ system will turn out to be crucial in determining which sub-amplitudes can contribute and what possible meson exchanges can take place. This will be discussed in considerable detail below.

In this first stage we explore the $dd \rightarrow \alpha\pi^0$ production process using chiral EFT with the simplest deuteron and α -particle wave functions, and ignoring the effects of initial-state interactions. This will give us an initial test of the amplitudes and provide us with the framework necessary to establish the ingredients for a full-fledged model. We are developing

a full model, using realistic wave functions and incorporating initial-state interactions, along with Δ admixtures, and the results will be reported in forthcoming papers.

The chiral power counting scheme is developed in Sec. II, resulting in a list of possible CSB amplitudes. Our simplified model is presented in Sec. III. The relative importance of the amplitudes in this model is investigated in Sec. IV. The paper then concludes in Sec. V with a discussion of the results, implications for the interpretation of the IUCF experiment, and future prospects. Some details of the calculation are included in an Appendix.

II. CSB OPERATORS

We use the EFT power-counting scheme to classify the CSB pion production operators in this section. In addition, the specific forms of the tree-level one- and two-body operators are derived. A few unknown low-energy constants LECs appear in the first few orders. Since these cannot be determined by symmetry considerations, we use phenomenological transition amplitudes to estimate their size. The effects of the derived operators are evaluated using a simplified model in Sec. III. This allows us to check that the leading non-vanishing operators of the chiral expansion indeed lead to a CSB cross section of the observed order of magnitude.

A. Effective Interactions

In QCD, the pseudo-Goldstone bosons of spontaneously broken chiral symmetry, $SU(2) \times SU(2) \rightarrow SU(2)$, can be identified with the pions. Chiral symmetry then strongly constrains the interactions allowed for pions with matter, and it is possible to construct a well-defined, convergent effective field theory for near-threshold pion reactions, namely chiral perturbation theory. Reviews with special emphasis on nucleon systems are provided in, e.g., Refs. [18, 19]. The chiral expansion can be adapted to the larger momentum scale inherent in pion production in nucleon-nucleon and nucleus-nucleus collisions [20, 21, 22, 23, 24]. The necessary power series may converge (albeit slowly) for this class of reactions [23, 24]. Studies of the $pp \rightarrow pp\pi^0$ reaction have shown that the resonance-saturation hypothesis does not necessarily lead to couplings of natural size, at least for interactions that contribute to the production of s -wave pions [21]. This issue should be further investigated.

We intend to reproduce the S -matrix elements of QCD at momenta much smaller than

the chiral-symmetry-breaking scale, here identified for simplicity with the nucleon mass M . To do this, the low-energy EFT must contain all the interactions among pions $\boldsymbol{\pi}$, nucleons N , and Delta-isobars Δ , that are allowed by the symmetries of QCD. For the following, the relevant CI interactions are

$$\begin{aligned}\mathcal{L}_{\text{CI}} = & -\frac{1}{4f_\pi^2}N^\dagger[\boldsymbol{\tau} \cdot (\boldsymbol{\pi} \times \dot{\boldsymbol{\pi}})]N + \frac{g_A}{2f_\pi}\left\{N^\dagger\boldsymbol{\tau} \cdot \vec{\sigma} \cdot N(\vec{\nabla}\boldsymbol{\pi}) - \frac{1}{2M}\left[iN^\dagger\boldsymbol{\tau} \cdot \dot{\boldsymbol{\pi}}\vec{\sigma} \cdot \vec{\nabla}N + h.c.\right]\right\} \\ & + \frac{h_A}{2f_\pi}\left\{N^\dagger\mathbf{T} \cdot \vec{S} \cdot \Delta(\vec{\nabla}\boldsymbol{\pi}) + h.c. - \frac{1}{M}\left[iN^\dagger\mathbf{T} \cdot \dot{\boldsymbol{\pi}}\vec{S} \cdot \vec{\nabla}\Delta + h.c.\right]\right\}. \end{aligned} \quad (1)$$

Here the first interaction is the Weinberg-Tomozawa term whose strength is fixed by chiral symmetry in terms of the pion decay constant $f_\pi = 92.4$ MeV. The other terms represent the standard axial-vector couplings — including recoil — of the pion to the nucleon (with $g_A = 1.26$) and to the Delta-isobar (with $h_A = 2.8$). Note that $\vec{\sigma}$ and $\boldsymbol{\tau}$ are the usual Pauli matrices in spin and isospin space, and \vec{S} and \mathbf{T} are the standard $N\Delta$ spin and isospin transition matrices, normalized such that $S_iS_j^+ = \frac{1}{3}(2\delta_{ij} - i\varepsilon_{ijk}\sigma_k)$, $T_aT_b^+ = \frac{1}{3}(2\delta_{ab} - i\varepsilon_{abc}\tau_c)$.

Charge symmetry breaking can occur either via exchange of a long-wavelength (soft) virtual photon or via short-range interactions. The former is generated by writing all allowed gauge-invariant interactions of the photon field. The latter are represented by local interactions that come either from the quark mass difference $m_u - m_d \equiv \epsilon(m_u + m_d)$, or from the exchange of short-wavelength (hard) photons (“indirect” electromagnetic effects), or both. The relevant CSB interactions are

$$\begin{aligned}\mathcal{L}_{\text{CSB}} = & \frac{\delta M}{2}N^\dagger\left(\tau_3 - \frac{\pi_3\boldsymbol{\tau} \cdot \boldsymbol{\pi}}{2f_\pi^2}\right)N + \frac{\bar{\delta}M}{2}N^\dagger\left(\tau_3 + \frac{\pi_3\boldsymbol{\tau} \cdot \boldsymbol{\pi} - \boldsymbol{\pi}^2\tau_3}{2f_\pi^2}\right)N \\ & - \frac{3\delta M}{8M^2}\left[N^\dagger\left(\tau_3 - \frac{\pi_3\boldsymbol{\tau} \cdot \boldsymbol{\pi}}{2f_\pi^2}\right)\nabla^2N + (\nabla^2N)^\dagger\left(\tau_3 - \frac{\pi_3\boldsymbol{\tau} \cdot \boldsymbol{\pi}}{2f_\pi^2}\right)N\right] \\ & - \frac{3\bar{\delta}M}{8M^2}\left[N^\dagger\left(\tau_3 + \frac{\pi_3\boldsymbol{\tau} \cdot \boldsymbol{\pi} - \boldsymbol{\pi}^2\tau_3}{2f_\pi^2}\right)\nabla^2N + (\nabla^2N)^\dagger\left(\tau_3 + \frac{\pi_3\boldsymbol{\tau} \cdot \boldsymbol{\pi} - \boldsymbol{\pi}^2\tau_3}{2f_\pi^2}\right)N\right] \\ & + \frac{1}{4M^2f_\pi^2}N^\dagger\left[-\delta M\nabla^2(\pi_3\boldsymbol{\tau} \cdot \boldsymbol{\pi}) + \bar{\delta}M\nabla^2(\pi_3\boldsymbol{\tau} \cdot \boldsymbol{\pi} - \boldsymbol{\pi}^2\tau_3)\right]N \\ & + \frac{1}{2M^2}i\varepsilon_{ijk}\left[-\delta M(\partial_iN)^\dagger(\pi_3\boldsymbol{\tau} \cdot \boldsymbol{\pi})\sigma_k\partial_jN + \bar{\delta}M(\partial_iN)^\dagger(\pi_3\boldsymbol{\tau} \cdot \boldsymbol{\pi} - \boldsymbol{\pi}^2\tau_3)\sigma_k\partial_jN\right] \\ & - \frac{(\beta_1 + \bar{\beta}_3)}{2f_\pi}\left\{N^\dagger\vec{\sigma}N \cdot \vec{\nabla}\pi_3 - \frac{1}{2M}\left[iN^\dagger\dot{\pi}_3\vec{\sigma} \cdot \vec{\nabla}N + h.c.\right]\right\} + \dots, \end{aligned} \quad (2)$$

where $\delta M = O(\epsilon m_\pi^2/M)$ and $\bar{\delta}M = O(\alpha M/\pi)$ are, respectively, the quark-mass-difference and electromagnetic contributions to the nucleon mass difference, and $\beta_1 = O(\epsilon m_\pi^2/M^2)$ and $\bar{\beta}_3 = O(\alpha/\pi)$ are, respectively, the quark-mass-difference and electromagnetic contributions

to the isospin-violating pion-nucleon coupling. This Lagrangian is consistent with the one from Ref. [20], with the $\bar{\delta}M$ term added from Ref. [33] and the pion-nucleon ($\beta_1 + \bar{\beta}_3$) term from Ref. [30]. This Lagrangian is also consistent with that of Ref. [30]. An apparent difference of an overall minus sign arises because Ref. [30] used different signs for the pion field and for $\delta M + \bar{\delta}M$. The CSB seagull term is consistent with the one used in Ref. [33]. These and other CSB EFT interactions were considered in Refs. [24, 26].

As usual, we have used [26] naive dimensional analysis to estimate the strengths of the terms in the Lagrangian, i.e., we have assumed that the LECs are of natural size. In principle, these parameters should be determined using experimental data. We now discuss some of the information we have about them.

The first two terms of Eq. (2) are the pion-nucleon seagull interactions required by chiral symmetry [26, 27] and can be described as the CSB components of the pion-nucleon σ -term. The strengths are determined by the coefficients δM and $\bar{\delta}M$, with their sum related to the nucleon mass splitting: to this order,

$$\delta M + \bar{\delta}M = \Delta M = M_n - M_p = 1.29 \text{ MeV.} \quad (3)$$

The coefficients are not well-known separately. With some assumptions about higher-energy physics, the Cottingham sum rule can be used to give $\bar{\delta}M = -(0.76 \pm 0.30)$ MeV [35]. It is desirable to determine these parameters without these assumptions. The δM , $\bar{\delta}M$ contribution to other observables generally depends on a different combination than that in Eq. (3). It is difficult to isolate the parameters in πN scattering, so it was suggested [33] that CSB in pion production could be used instead. The forward-backward asymmetry in $np \rightarrow d\pi^0$ was shown to be sensitive to $\delta M - \bar{\delta}M/2$, but it also depends significantly on $\beta_1 + \bar{\beta}_3$.

The other LECs are not well-known either. The pion-nucleon CSB parameter $\beta_1 + \bar{\beta}_3$ is constrained by the Nijmegen phase-shift analysis of the NN scattering data [36] to be $\beta_1 + \bar{\beta}_3 = (0 \pm 9) \times 10^{-3}$ [30]. Below we estimate the impact of this interaction following the standard practice of neglecting $\bar{\beta}_3$ and modeling β_1 by π - η mixing [30], which is consistent with the bound from NN scattering.

Among the “...” in Eq. (2) there are several CSB short-range pion–two-nucleon interactions that contribute in the order we will be considering. One example is

$$- \frac{(\gamma_1 + \bar{\gamma}_3)}{2f_\pi} N^\dagger N \left\{ N^\dagger \vec{\sigma} N \cdot \vec{\nabla} \pi_3 - \frac{1}{2M} [iN^\dagger \dot{\pi}_3 \vec{\sigma} \cdot \vec{\nabla} N + h.c.] \right\}, \quad (4)$$

where we expect that $\gamma_1 = O[\epsilon m_\pi^2/(f_\pi^2 M^3)]$ and $\bar{\gamma}_3 = O[\alpha/(\pi f_\pi^2 M)]$, for the quark-mass-difference and electromagnetic contributions respectively. We know very little about the LECs appearing in these short-range pion–two-nucleon interactions, and therefore will model these LECs with various heavy-meson-exchange HME mechanisms as detailed below.

B. Power Counting

It is necessary to order the various amplitudes according to the size of their expected contributions to pion production. There are several strong-interaction scales in the problem, namely,

- $\chi = p/M \sim \sqrt{m_\pi/M}$, the initial c.m. momentum of the deuteron divided by the chiral-symmetry-breaking scale (here identified with the nucleon mass M), which we will use as the expansion parameter;
- $m_\pi/M \sim \chi^2$, where m_π denotes the pion mass;
- $(M_\Delta - M)/M \sim \chi$, with M_Δ the Delta mass [51] — the order assignment given is in line with Ref. [24]; and
- $\gamma/M \sim \chi^2$, where γ is the typical nucleon momentum inside the deuteron and the α particle (for simplicity we will not distinguish between the two).

Moreover, the strengths of CSB effects are governed by

- α/π , the fine structure constant that appears with every exchange of a virtual photon, typically with an extra factor of π ; and
- $\epsilon m_\pi^2/M^2$, the factors of $m_u - m_d$ that come from explicit chiral symmetry breaking via quark-mass terms [52].

We discuss the two types of contributions individually, to first order, in the following subsections. Second-order effects in α and ϵ can also be treated, but are truly small, and ignored here.

Power counting in systems of two or more nucleons is complicated by the fact that some diagrams contain small energy denominators, corresponding to states that differ from initial and/or final states only by an energy $O(\gamma^2/M)$. Sub-diagrams that do not contain such

enhancements are denoted as irreducible. Conservation of energy and momentum in pion production requires that at least one interaction takes place among nucleons — before, during, or after the pion emission. This interaction transfers a momentum of order $p \sim \sqrt{m_\pi M}$. When such interactions happen before or after pion emission, they are included in the (high-momentum tail of the) initial- or final-state wave function. In this case we can speak of a “one-body” pion-emission operator. However, in order to compare sub-amplitudes of the same dimensions and count powers of χ , we include these interactions as part of the irreducible pion sub-amplitude. The full pion-production amplitude is “reducible”, because it includes further initial- and final-state interactions (via the deuteron and α wave functions) that transfer momenta of order γ .

The separation of reducible and irreducible sub-amplitudes is convenient because it isolates interactions involving the scale χ in the irreducible part. Power counting for the initial- and final-state interactions corresponding to momenta of $O(\gamma)$ can be done in the usual way [19]. In this first paper, we use simple wave functions *in lieu* of wave functions obtained in EFT. The needed EFT wave functions may soon be a reality, since chiral three- and four-nucleon calculations already exist [37].

The loop integrals, propagators and vertices bring factors of momenta, masses, and coupling constants to any given diagram. Dimensional analysis can be used to express any coupling constant as appropriate powers of M times numbers of order 1 (for CI operators) or $\epsilon m_\pi^2/M^2$ or α/π (for CSB operators). Some factors, common to all diagrams, are not written explicitly. For example, since we study a system of four nucleons that are bound in an α particle in the final state, there are always three loops that are controlled by γ . Thus, all we need to keep explicitly for a $2n$ -nucleon operator (in addition to what can be read from the vertices and propagators directly) is a common factor $(p^3/(4\pi)^2)^{(n-1)}$ (here we have only a three-dimensional integral because we estimate the measure of a convolution integral with a wave function). Therefore explicit factors of γ are not included explicitly in the assignments of chiral order.

As stressed in Refs. [23, 24], the hierarchy of diagrams is very different for s -wave pions and p -wave pions. We here specialize to s -wave pion production, relevant for the recent IUCF experiment.

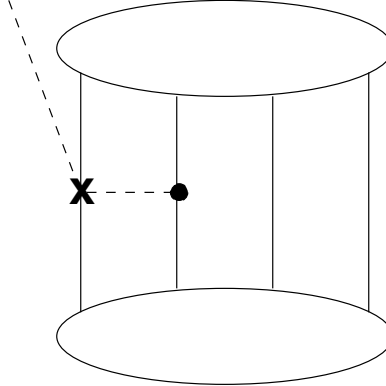


FIG. 1: Leading order diagram with strong CSB. The cross indicates the occurrence of CSB. The dot represents a leading-order CI vertex.

1. Diagrams proportional to ϵ

At leading order LO there is only one contribution: pion rescattering, where the CSB occurs through the seagull pion-nucleon terms linked to the nucleon mass splitting — see Fig. 1, in which the leading CI interaction is represented by a dot, and CSB by a cross. The irreducible part of this diagram is $O[\epsilon m_\pi^2/(f_\pi^3 M_p)]$. The analogous diagram was identified in Ref. [33], using the present counting scheme, as giving the dominant contribution to the forward-backward asymmetry in $np \rightarrow d\pi^0$. We shall show that, in the dd induced CSB reaction, selection rules tend to suppress the rescattering via these seagull terms, if initial state interactions are ignored.

There is no next-to-leading order NLO contribution (suppressed by just one power of χ). At NNLO, however, there are several contributions, displayed in Fig. 2. The encircled vertices stem from sub-leading Lagrange densities. For example, the sub-leading vertex in diagrams (a) and (b) arises from the recoil correction of the CSB πNN vertex, the one in diagram (c) denotes the recoil correction of the CI πNN vertex, and that in diagram (d) represents the recoil corrections to the CSB seagulls. Diagram (b) involves the Weinberg-Tomozawa vertex.

Note that diagram (a) can be interpreted as the sandwich of a one-body CSB operator between CI initial- and final-state wave functions. It is necessary to include the effects of CSB in the wave functions in addition to the diagrams shown in Fig. 2. The easiest way to see this is to compare the size of the LO CSB production operator (rescattering via the

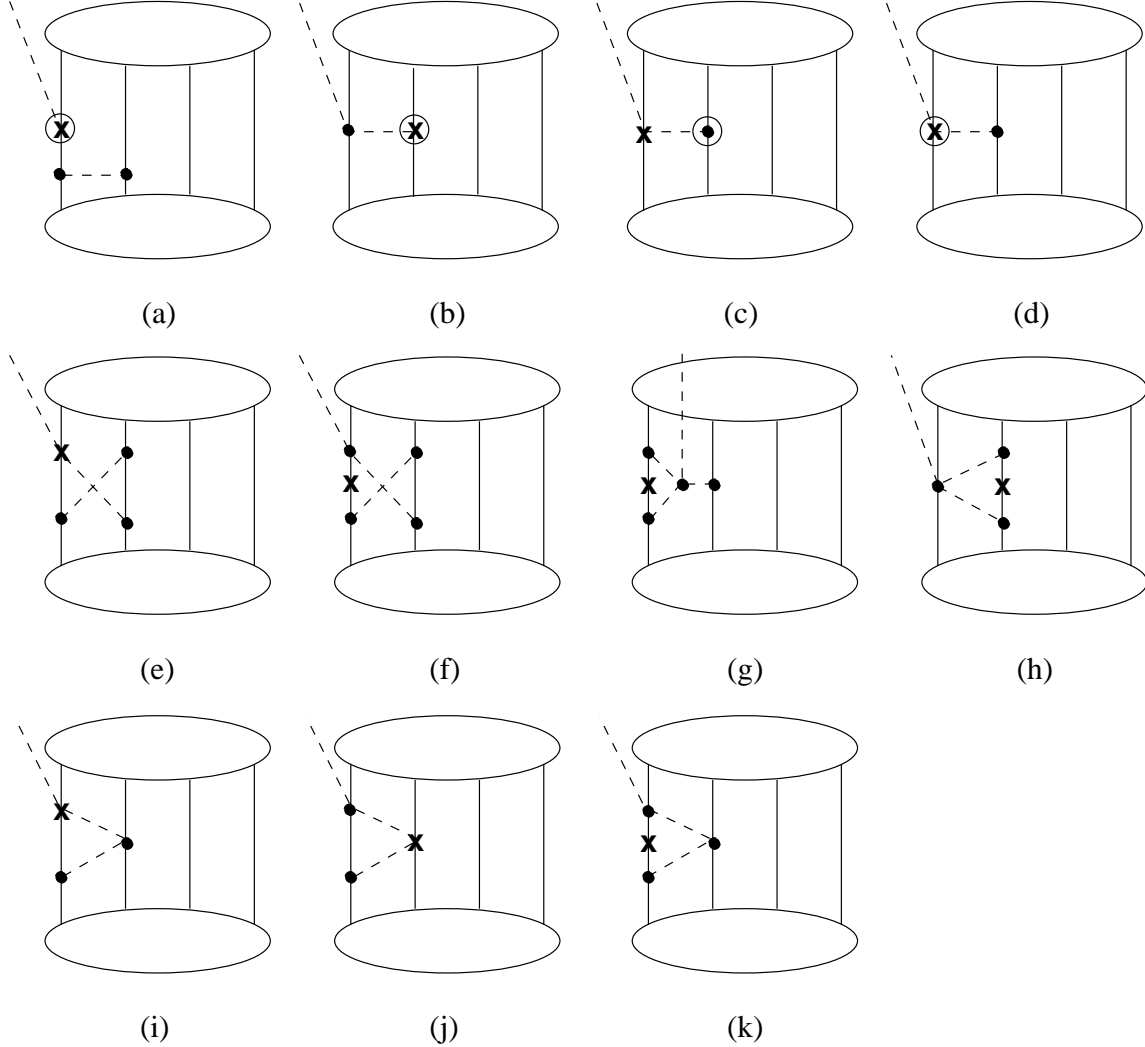


FIG. 2: NNLO diagrams with strong CSB. Vertices with an additional circle originate from sub-leading Lagrange densities. We do not display all possible orderings.

seagull terms) times the LO CI contribution to the NN potential (e.g., one-pion exchange) with the LO CI production operator (rescattering via the Weinberg-Tomozawa term) times the LO CSB contribution to the NN scattering — assumed to be one-pion exchange with a CSB coupling on one vertex. This shows that CSB in the wave functions should be significant in a NNLO calculation. Typical diagrams are shown in Fig. 3.

The effects of parity conservation suppress the influence of CSB in a single deuteron wave function, but CSB does occur in the interactions between the deuterons. One such term arises from photon exchange as in Fig. 3. The dominant CSB contribution in the α -particle wave function may be expressible in terms of the point radius difference of the neutron and

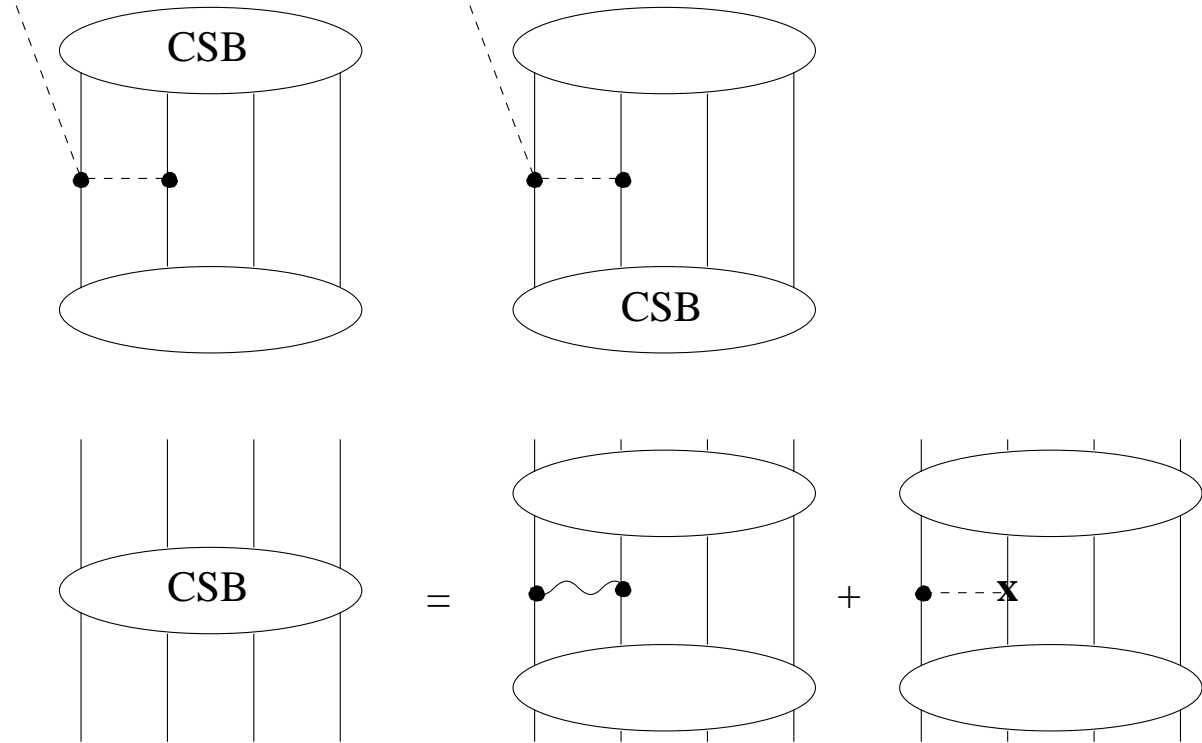


FIG. 3: The influence of strong and electromagnetic CSB in the initial and final state. The wiggly line represents the exchange of a photon, while the dashed line represents a meson exchange contribution with one CSB vertex.

proton $r_n - r_p$, which can be calculated in microscopic models for few-body systems. Results of these calculations will be presented in future work.

Loop diagrams appear already at NNLO. We display only the topology of these diagrams, but it is clearly necessary to include all other orderings. A striking feature of the present analysis is that, at this order, no counterterms are allowed by the symmetries. The corresponding counterterms — the CSB four-nucleon contact interactions in Eq. (2), displayed below in Fig. 4(b), appear first at N^4LO . Therefore, those parts of the loops that appear at NNLO are to be finite. This situation is in complete analogy to the CI pion production in nucleon-nucleon collisions discussed in detail in Ref. [24].

Fig. 4 displays some of the higher-order contributions. A contribution with an intermediate Δ -isobar, that appears at N^3LO , is shown in diagram (a). The CSB contact interactions displayed in diagram (b) start to contribute at N^4LO . Their values will be estimated below using phenomenological input.

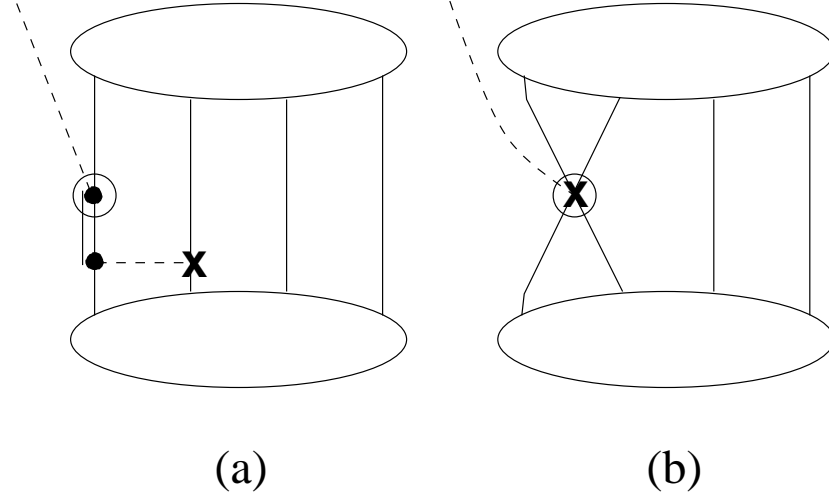


FIG. 4: Some typical higher-order diagrams with strong CSB. A double line represents a Δ -isobar. Diagram a) appears at N^3LO whereas diagram b) is a N^4LO contribution.

2. Diagrams proportional to α

Electromagnetic contributions can be ordered relative to each other in exactly the same fashion. In this case, the LO is $O[\alpha M/(4\pi f_\pi^3 p)]$. These diagrams contain Coulomb interactions in the initial- or final-state. In particular, the effects of photon exchange between the initial deuterons, followed by production by a strong interaction, could be very important. An example of such a term is provided by Fig. 3.

The NLO electromagnetic diagrams — suppressed by one power of χ — that contribute to CSB in the production operator are shown in Fig. 5. It is important to note that in threshold kinematics (on the two-body level the outgoing nucleons as well as the produced pion are at rest) the two diagrams (b) and (c) cancel — in a realistic calculation we should expect some of this cancellation effect to survive. The three-body diagram (a) should therefore be the one to estimate the photon effects in the production operator at this order. In addition, higher-order photon couplings in the wave functions contribute at this order.

There are various other contributions at NNLO — see Fig. 6. In what follows we will explicitly calculate the two-body operator that involves a photon exchange stemming from gauging the recoil correction to the πNN vertex [53], diagram (a). This will give us an idea of the relative importance of soft photons compared to the strong CSB effects.

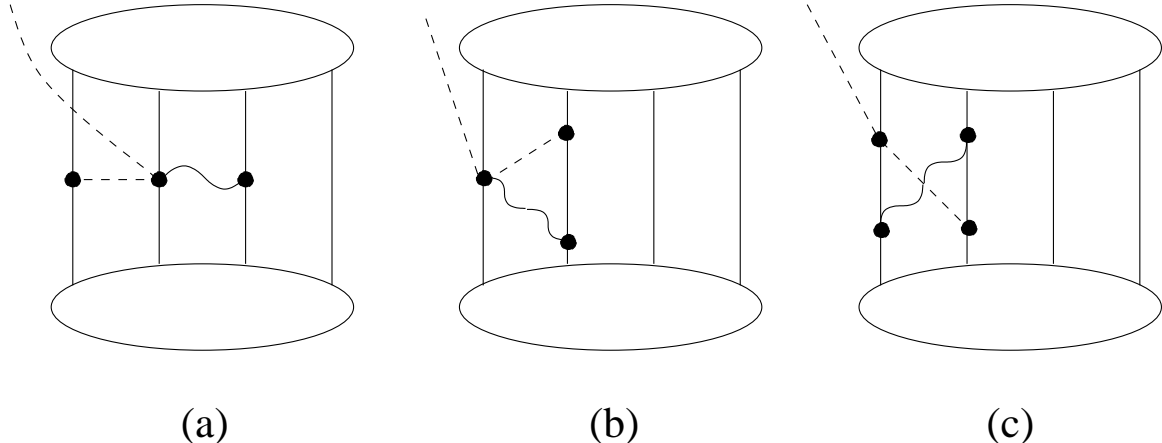


FIG. 5: NLO diagrams with CSB stemming from soft photons.

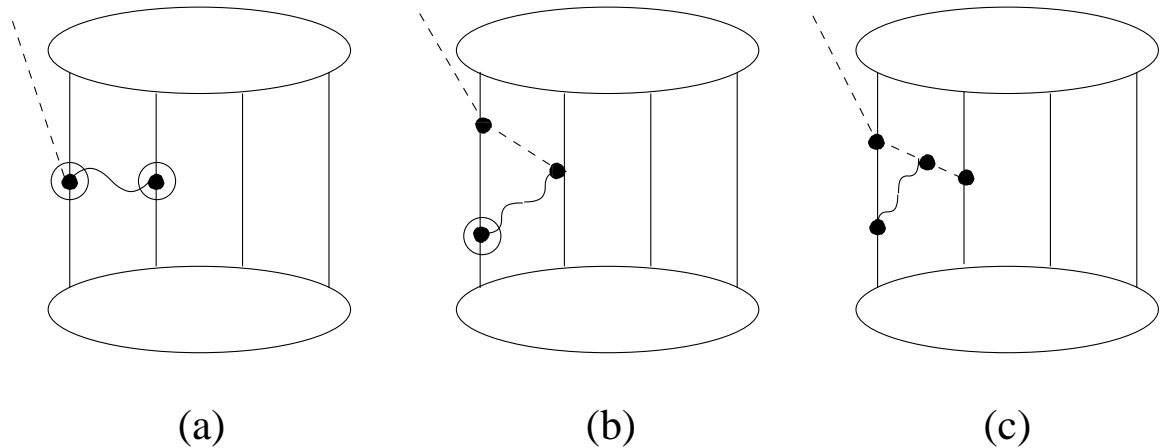


FIG. 6: NNLO diagrams with CSB stemming from soft photons.

C. Heavy-Meson Interactions

We assume that EFT LECs can be determined using the exchange of massive resonances to estimate the impact of short-range physics. Such an approach was used in CI pion production, for example, in Refs. [20, 21]. In principle the counterterms can be determined by other data, and this would eliminate the need for our heavy-meson model. In the present context, we include the exchanges of the (σ , ω , and ρ) mesons depicted in Fig. 7.

The meson-exchange diagrams can be calculated from the following Lagrangian:

$$\mathcal{L}_{\text{HME}} = -ig_\eta \bar{\psi} \gamma_5 \psi \eta + g_\sigma \bar{\psi} \psi \sigma - g_\omega \bar{\psi} \gamma_\mu \psi \omega^\mu - g_\rho \bar{\psi} \boldsymbol{\tau} \cdot \left[\gamma_\mu \boldsymbol{\rho}^\mu + C_\rho \frac{\sigma_{\mu\nu}}{2M} \partial^\mu \boldsymbol{\rho}^\nu \right] \psi. \quad (5)$$

Here ψ is the Dirac four-component nucleon field and η , σ , ω^μ , $\boldsymbol{\rho}^\mu$ are the meson fields. We use the parameter values in Table I as representative of typical one-boson exchange OBE

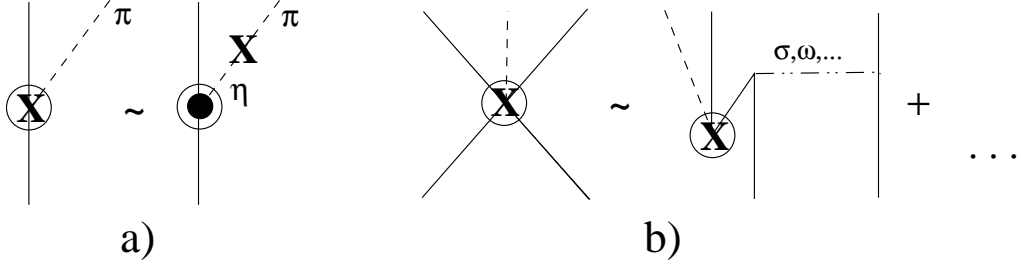


FIG. 7: Resonance saturation for (a) the CSB πNN vertex modeled here by π - η mixing and (b) the CSB four-nucleon operators. The ellipsis indicate that additional short-range mechanisms are to be included, as discussed in the text.

models [38] and the standard value $C_\rho = 6.1$ for the large ratio of tensor $\sigma_{\mu\nu}\partial^\mu/(2M)$ to vector γ_μ coupling for the ρ meson. The η -nucleon coupling g_η will be discussed below.

TABLE I: Table of meson masses and coupling constants.

	m (MeV/ c^2)	$\frac{g_{xNN}^2}{4\pi}$
σ	550	7.1
ω	783	10.6
ρ	770	0.43

The photon-nucleon coupling is described by the Lagrangian (up to dimension 5)

$$\mathcal{L}_\gamma = -e\bar{\psi} \left[\frac{1+\tau^3}{2} \gamma_\mu A^\mu + \left(\frac{\lambda_0 + \lambda_1 \tau^3}{2} \right) \frac{\sigma_{\mu\nu}}{2M} \partial^\mu A^\nu \right] \psi, \quad (6)$$

where $\lambda_{0,1} = \lambda_p \pm \lambda_n$ and $\lambda_p = 1.793$ and $\lambda_n = -1.913$ are the proton and neutron anomalous magnetic moments.

D. Explicit form of leading tree-level operators

We now turn to the explicit form of the leading tree-level two-body operators, in order to exploit the selection rules. Corresponding expressions for the loops as well as the three-body electromagnetic term mentioned above will be presented in a subsequent publication.

We start with the formally leading mechanism, Fig. 1, together with the recoil correction at the pion-nucleon vertex, Fig. 2(c). The pion-exchange operator coming from the seagull

terms is

$$\begin{aligned}\mathcal{O}_\pi &= \frac{1}{4f_\pi^2} [\delta M(\boldsymbol{\tau}_i \cdot \boldsymbol{\tau}_j + \tau_i^3 \tau_j^3) - \bar{\delta} M(\boldsymbol{\tau}_i \cdot \boldsymbol{\tau}_j - \tau_i^3 \tau_j^3)] \\ &\quad \times \sum_{i \neq j} \boldsymbol{\sigma}_i \cdot \left[(\mathbf{k}'_i f_{ij}^\pi - f_{ij}^\pi \mathbf{k}_i) - \frac{q_i^0}{2M} (\mathbf{k}'_i f_{ij}^\pi + f_{ij}^\pi \mathbf{k}_i) \right],\end{aligned}\quad (7)$$

$$f_{ij}^\pi = \frac{g_A}{2f_\pi} \frac{e^{-\mu r_{ij}}}{4\pi r_{ij}}, \quad (8)$$

where $\mathbf{r}_{ij} = \mathbf{r}_i - \mathbf{r}_j$ is the relative coordinate of nucleons i and j , $\mathbf{k}_i = -i \vec{\nabla}_i$ ($\mathbf{k}'_i = i \vec{\nabla}_i$) is the initial (final) momentum of nucleon i , $\mathbf{q}_i = \mathbf{k}'_i - \mathbf{k}_i$ is the momentum transfer to nucleon i (here symmetrized with the Yukawa factor), and the Yukawa parameter $\mu = \sqrt{\frac{3}{4}} m_\pi$. In our numerical estimates below, we use the value for $\bar{\delta} M$ from the Cottingham sum rule, which translates into $\delta M - \bar{\delta} M/2 = 2.4$ MeV [33]. In the fixed kinematics approximation for pion production by two nucleons, the exchange pion energy $q_i^0 = m_\pi/2$ [39].

It may be noted that the term from Eq. (8), proportional to \mathbf{q}_i , actually gives rise to most of the CSB s -wave amplitude in $np \rightarrow d\pi^0$ [33]. This interferes with CI p -wave production. On the other hand, the CSB p -wave amplitude, arising mainly from the CSB one-body operator shown in Eq. (9) or from a CI production operator following a CSB initial state interaction, interferes with the CI s -wave and was about as important in Ref. [33], but would be relatively irrelevant here in the absence of such an important interference at threshold.

The nucleon recoil term $\sim \frac{1}{2}(\mathbf{k}'_i + \mathbf{k}_i)$ is smaller, since it is suppressed by an additional factor m_π/M . However, if the simple deuteron and α wave functions of Sec. III are used, the spin-isospin symmetries prohibit this amplitude for nucleons from different deuterons. The \mathbf{q}_i term will integrate to zero inside a single deuteron, leaving the (in-deuteron) recoil as the only allowed contribution. Thus the symmetries in this particular model suppress the contribution from Fig. 1, leaving only Fig. 2(c): the seagull amplitude is reduced from LO to NNLO and there is no momentum sharing. This suppression is expected to be less important once initial state interactions are included and realistic wave functions are used.

At NNLO there are various other contributions. The one-body operator, Fig. 2(a), is

$$\mathcal{O}_1 = \frac{\beta_1}{2f_\pi} \sum_i \boldsymbol{\sigma}_i \cdot \left(\mathbf{q}_i - \frac{\omega}{2M} (\mathbf{k}'_i + \mathbf{k}_i) \right) \rightarrow \Lambda_1 \frac{1}{2} \sum_i \boldsymbol{\sigma}_i \cdot (\mathbf{k}'_i + \mathbf{k}_i), \quad (9)$$

$$\Lambda_1 = -\frac{\beta_1}{2f_\pi} \frac{\omega}{M}. \quad (10)$$

The p -wave $\mathbf{q}_i = -\mathbf{p}_\pi$ term is suppressed in the threshold regime considered. In addition, it is not allowed in our plane wave approximation, since it lacks the tensor coupling required

for the $^5D_1 p$ transition. The s -wave recoil term is allowed, albeit suppressed by a factor ω/M , hence the parameter Λ_1 . This s -wave term is NNLO.

The isospin-violating β_1 is here modeled [30] by π - η mixing [see Fig. 7(a)],

$$\beta_1 = \bar{g}_\eta \langle \pi^0 | H | \eta \rangle / m_\eta^2, \quad (11)$$

where $\bar{g}_\eta = g_\eta f_\pi / M = 0.25$ is the ηNN coupling constant and $\langle \pi^0 | H | \eta \rangle = -4200 \text{ MeV}^2$ the π - η -mixing matrix element [40]. The value of \bar{g}_η corresponds to $g_\eta^2 / 4\pi = 0.51$, similar to the small values found from photo-production experiments [41]. However, other values, based on hadronic experiments, are as high as $g_\eta^2 / 4\pi = 3.68$ [42] or 2–7 for the OBE parameterizations of the Bonn potentials [43]. The CD-Bonn OBE potential assumes a vanishing value for g_η , since in the full Bonn model no explicit η contribution was required by the NN data [44]. Furthermore, the value of the π - η -mixing matrix element is uncertain. With our particular choice we get $\beta_1 = -3.5 \times 10^{-3}$ [30]. Using $g_\eta^2 / 4\pi = 3.68$ and $\langle \pi^0 | H | \eta \rangle = -5900 \text{ MeV}^2$, as done in Ref. [33], gives $\beta_1 = -1.2 \times 10^{-2}$.

One important issue is the relative sign of this contribution, which is apparently not determined experimentally. The sign given above is consistent with $SU(3) \times SU(3)$ chiral perturbation theory, which can be formulated in terms of a pseudoscalar octet π_a and a baryon octet. The sign of the π_3 - π_8 mixing is, in leading order, fixed by $m_u - m_d$. The interactions of π_3 and π_8 with the nucleon are determined by the standard weak couplings D and F , which are fixed in weak decays. With our definitions of g_A , \bar{g}_η , and β_1 given above and the values of D and F given, e.g., in Ref. [45], we find $g_A > 0$ if we define $\pi_3 = \pi^0$, $g_\eta > 0$ and $\langle \pi^0 | H | \eta \rangle < 0$, so that $\beta_1 < 0$. This conclusion holds, as it should, regardless of the sign definition of η , that is, whether one takes η as π_8 or $-\pi_8$.

Fig. 2(b) represents the process where a CSB one-body operator produces a charged pion which then changes into a neutral pion as it re-scatters on another nucleon via the CI Weinberg-Tomozawa term. This contribution is small in $dd \rightarrow \alpha\pi^0$, since the isospin couplings force the pion exchange to occur inside one of the deuterons. This is a situation very similar to the seagull CSB terms, which was discussed above, but with a smaller coefficient. Note that a similar diagram where the exchanged pion is neutral is also small, since the on-shell $\pi^0 N \rightarrow \pi^0 N$ amplitude receives contributions only at one order higher than that from the Weinberg-Tomozawa term. Since the operator in Fig. 2(d) is a relativistic correction to the leading order pion rescattering, it has exactly the same spin-isospin structure (except its

last term) as can be seen in Eq. (2). Thus its first few terms are also confined to in-deuteron exchanges and since they are already suppressed by two orders $(k_i/M)^2 \sim m_\pi/M$, these terms are negligible. The last $\delta M/\bar{\delta}M$ term has an extra Pauli spin matrix and can possibly be important since this may allow for momentum sharing. However, this term always includes the momentum of a final nucleon, which is very small near the pion threshold and this NNLO amplitude is likely to be suppressed as well. We will not consider these operators any further.

The pion loops in Fig. 2(e-k) represent long-range, non-analytic contributions as well as short-range, analytic effects. The latter cannot be separated from the short-range contributions of Fig. 4(b), originating from a four-nucleon–pion CSB contact interaction. In this first study, we limit ourselves to an estimate of these effects via resonance saturation from various heavy-meson exchange currents HMECs — see Fig. 7(b). In the case of the $pp \rightarrow pp\pi^0$ reaction, heavy-meson exchanges involving the creation of a nucleon–anti-nucleon pair (z-graphs) were shown to be important for the total (CI) cross section near threshold [21, 46, 47]. These exchanges correspond to contact interactions in the EFT [20, 21]. Here, we include the analogous CSB interactions where CSB occurs in the pion emission or in the meson exchange.

The HME two-body operators are derived directly from a low-energy reduction of the Feynman rules for the HME Lagrangian Eq. (5). This gives the σ -meson–exchange two-body operator

$$\mathcal{O}_\sigma = \Lambda_1 \frac{1}{2} \sum_{i \neq j} \boldsymbol{\sigma}_i \cdot (\mathbf{k}'_i f_{ij}^\sigma + f_{ij}^\sigma \mathbf{k}_i), \quad (12)$$

$$f_{ij}^\sigma = \frac{g_\sigma^2}{4\pi M} \frac{e^{-m_\sigma r_{ij}}}{r_{ij}}, \quad (13)$$

where only the symmetrized recoil term has been used. Note that the sum is over $i \neq j$ rather than $i < j$.

The ω -exchange two-body operator is

$$\mathcal{O}_\omega = -\Lambda_1 \frac{1}{2} \sum_{i \neq j} \left[\boldsymbol{\sigma}_j \cdot (\mathbf{k}'_i f_{ij}^\omega + f_{ij}^\omega \mathbf{k}_i) + i(\boldsymbol{\sigma}_i \times \boldsymbol{\sigma}_j) \cdot (\mathbf{k}'_j f_{ij}^\omega - f_{ij}^\omega \mathbf{k}_j) \right], \quad (14)$$

$$f_{ij}^\omega = \frac{g_\omega^2}{4\pi M} \frac{e^{-m_\omega r_{ij}}}{r_{ij}}. \quad (15)$$

Note this has an overall minus sign and $\boldsymbol{\sigma}_j$ instead of $\boldsymbol{\sigma}_i$ compared to \mathcal{O}_σ . Finally there is a new term involving the momentum transferred to nucleon j .

The ρ -exchange two-body operator is

$$\mathcal{O}_\rho = -\Lambda_1 \frac{1}{2} \sum_{i \neq j} \boldsymbol{\tau}_i \cdot \boldsymbol{\tau}_j \left[\boldsymbol{\sigma}_j \cdot (\mathbf{k}'_i f_{ij}^\rho + f_{ij}^\rho \mathbf{k}_i) + i(1 + C_\rho) (\boldsymbol{\sigma}_i \times \boldsymbol{\sigma}_j) \cdot (\mathbf{k}'_j f_{ij}^\rho - f_{ij}^\rho \mathbf{k}_j) \right], \quad (16)$$

$$f_{ij}^\rho = \frac{g_\rho^2}{4\pi M} \frac{e^{-m_\rho r_{ij}}}{r_{ij}}. \quad (17)$$

The ρ HMEC is of order of the small vector times the large tensor coupling constant and has no contributions of order of the tensor coupling squared.

The ρ - ω -mixing two-body operator is

$$\mathcal{O}_{\rho-\omega} = -\Lambda_{\rho-\omega} \frac{1}{2} \sum_{i \neq j} \left\{ (1 + \tau_i^3 \tau_j^3) \boldsymbol{\sigma}_j \cdot (\mathbf{k}'_i f_{ij}^{\rho\omega} + f_{ij}^{\rho\omega} \mathbf{k}_i) \right. \quad (18)$$

$$\left. + i[1 + \tau_i^3 \tau_j^3 (1 + C_\rho)] (\boldsymbol{\sigma}_i \times \boldsymbol{\sigma}_j) \cdot (\mathbf{k}'_j f_{ij}^{\rho\omega} - f_{ij}^{\rho\omega} \mathbf{k}_j) \right\}, \quad (19)$$

$$\Lambda_{\rho-\omega} = -\frac{g_A}{2f_\pi} \frac{\omega}{M} \left(\frac{\langle \rho | H | \omega \rangle}{m_\omega^2} \right), \quad (20)$$

$$f_{ij}^{\rho\omega} = \frac{g_\rho g_\omega}{4\pi M r_{ij}} \frac{m_\omega^2}{m_\omega^2 - m_\rho^2} (e^{-m_\rho r_{ij}} - e^{-m_\omega r_{ij}}), \quad (21)$$

where the ρ - ω mixing is given by $\langle \rho | H | \omega \rangle = -4300 \text{ MeV}^2$ [40]. A somewhat smaller number ($\langle \rho | H | \omega \rangle = -3500 \pm 300 \text{ MeV}^2$) was obtained in a more recent analysis [48]. The isospin-independent part of this ρ - ω operator is only of the order of the small ρ vector coupling. Note, however, that there is a $\tau_i^3 \tau_j^3$ term that involves the large ρ tensor coupling.

At momenta much smaller than the heavy-meson masses these HMECs are equivalent to short-range pion–two-nucleon contact interactions, with specific values for the LECs. For example, the σ mechanism [Eq. (13)] goes into the interaction shown in Eq. (4) with γ_1 given by $\beta_1 g_\sigma^2 / (4\pi m_\sigma^2 M)$, which is consistent with the naive dimensional estimates.

In addition, we need to consider contributions from soft photons. There is a Coulomb interaction and a magnetic interaction (Fig. 3), and a three-body term [Fig. 5(a)]. As a first estimate, we shall compute the lowest order two-body diagram with a photon. This appears at NNLO and is shown in Fig. 6(a).

The soft photon exchange gives a structure very similar to that of ρ^0 - ω mixing:

$$\mathcal{O}_\gamma = -\Lambda_\gamma \frac{1}{2} \sum_{i \neq j} \left\{ (1 + \tau_i^3 \tau_j^3) \boldsymbol{\sigma}_j \cdot (\mathbf{k}'_i f_{ij}^\gamma + f_{ij}^\gamma \mathbf{k}_i) \right. \quad (22)$$

$$\left. + i[1 + \lambda_0 + (1 + \lambda_1) \tau_i^3 \tau_j^3] (\boldsymbol{\sigma}_i \times \boldsymbol{\sigma}_j) \cdot (\mathbf{k}'_j f_{ij}^\gamma - f_{ij}^\gamma \mathbf{k}_j) \right\},$$

$$\Lambda_\gamma = \frac{1}{4} \frac{g_A}{2f_\pi} \frac{\omega}{M}, \quad (23)$$

$$f_{ij}^\gamma = \frac{\alpha}{M r_{ij}}. \quad (24)$$

Note that the structure of this term is a consequence of gauge invariance, and this is why no new unknown parameters are introduced.

III. SIMPLIFIED MODEL

The interferences and relative importance of the CSB amplitudes of the previous section can be estimated in a simplified model, using a plane-wave approximation and the simplest possible d and α bound-state wave functions, those of a Gaussian form. A Feynman diagram for this model can be drawn as in Fig. 8. Assuming spatially-symmetric bound-state wave functions, the invariant amplitude is given by

$$\mathcal{M} = \int d^3r d^3\rho_1 d^3\rho_2 \langle A | \mathcal{O} | DD \rangle, \quad (25)$$

$$|A\rangle = \sqrt{2E_\alpha} \Psi_\alpha(r, \rho_1, \rho_2) |\alpha\rangle, \quad (26)$$

$$|DD\rangle = \sqrt{s} \Phi_d(\rho_1) \Phi_d(\rho_2) |dd\rangle, \quad (27)$$

where Ψ_α and Φ_d are the spatial parts of the α -particle and deuteron bound-state wave functions, and $s = 4E_d^2$ is the total c.m. energy squared. The ket vectors $|\alpha\rangle$ and $|dd\rangle$ contain the fully anti-symmetrized spin and isospin wave functions. Because of the symmetry requirements, the plane-wave dd scattering wave function is included in $|dd\rangle$ as given by Eqs. (34) and (35) below. The invariant amplitude can then be written as

$$\mathcal{M} = \sqrt{2E_\alpha s} \int d^3r d^3\rho_1 d^3\rho_2 \Psi_\alpha^\dagger(r, \rho_1, \rho_2) \langle \alpha | \mathcal{O} | dd \rangle \Phi_d(\rho_1) \Phi_d(\rho_2), \quad (28)$$

where $\langle \alpha | \mathcal{O} | dd \rangle$ contains all the spin-isospin couplings of the nucleons and the pion production operator \mathcal{O} .

The wave functions are expressed in terms of the (2+2) Jacobian coordinates

$$\begin{aligned} \mathbf{R} &= \frac{1}{4}(\mathbf{r}_1 + \mathbf{r}_2 + \mathbf{r}_3 + \mathbf{r}_4) \quad (\equiv 0 \text{ in c.m.}), \\ \mathbf{r} &= \frac{1}{2}(\mathbf{r}_1 + \mathbf{r}_2 - \mathbf{r}_3 - \mathbf{r}_4), \\ \boldsymbol{\rho}_1 &= \mathbf{r}_1 - \mathbf{r}_2, \\ \boldsymbol{\rho}_2 &= \mathbf{r}_3 - \mathbf{r}_4, \end{aligned} \quad (29)$$

with the corresponding momenta

$$\mathbf{K} = \mathbf{k}_1 + \mathbf{k}_2 + \mathbf{k}_3 + \mathbf{k}_4 \quad (\equiv 0 \text{ in c.m.}),$$

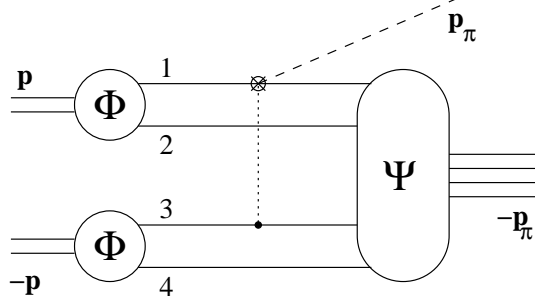


FIG. 8: Feynman diagram for pion production in the $dd \rightarrow \alpha\pi^0$ reaction, indicating the labeling of nucleons and defining basic kinematic variables.

$$\begin{aligned}
 \mathbf{k} &= \frac{1}{2}(\mathbf{k}_1 + \mathbf{k}_2 - \mathbf{k}_3 - \mathbf{k}_4) = \frac{1}{2}(\mathbf{p}_1 - \mathbf{p}_2) \ (\equiv \mathbf{p} \text{ in c.m.}), \\
 \boldsymbol{\kappa}_1 &= \frac{1}{2}(\mathbf{k}_1 - \mathbf{k}_2), \\
 \boldsymbol{\kappa}_2 &= \frac{1}{2}(\mathbf{k}_3 - \mathbf{k}_4),
 \end{aligned} \tag{30}$$

defined so that $\sum_i \mathbf{k}_i \cdot \mathbf{r}_i = \mathbf{K} \cdot \mathbf{R} + \mathbf{k} \cdot \mathbf{r} + \boldsymbol{\kappa}_1 \cdot \boldsymbol{\rho}_1 + \boldsymbol{\kappa}_2 \cdot \boldsymbol{\rho}_2$. The Jacobians are equal to unity in both representations.

The Gaussian functions that represent the ground state wave functions are explicitly expressed in these coordinates using $\sum_{i < j} (\mathbf{r}_i - \mathbf{r}_j)^2 = 4\mathbf{r}^2 + 2\boldsymbol{\rho}_1^2 + 2\boldsymbol{\rho}_2^2$:

$$\Psi_\alpha(r, \rho_1, \rho_2) = \frac{8}{\pi^{9/4} \alpha^{9/2}} \exp\left[-\frac{1}{\alpha^2} (2r^2 + \rho_1^2 + \rho_2^2)\right], \tag{31}$$

$$\Phi_d(\rho) = \frac{1}{\pi^{3/4} \beta^{3/2}} \exp\left(-\frac{1}{2\beta^2} \rho^2\right), \tag{32}$$

where the parameter values $\alpha = 2.77$ fm and $\beta = 3.189$ fm are derived from measured α and d rms point radii; $\langle r_\alpha^2 \rangle^{1/2} = 1.47$ fm and $\langle r_d^2 \rangle^{1/2} = 1.953$ fm [49].

Since we have assumed that the orbital parts of the wave functions are symmetric under the exchange of any pair of nucleons, we may define the initial- and final-state spin-isospin wave functions as

$$|\alpha\rangle = \frac{1}{\sqrt{2}} \{ ((1, 2)_1, (3, 4)_1)_0 [[1, 2]_0, [3, 4]_0]_0 - ((1, 2)_0, (3, 4)_0)_0 [[1, 2]_1, [3, 4]_1]_0 \}, \tag{33}$$

$$|dd\rangle = \frac{1}{\sqrt{3}} (1 - P_{23} - P_{24}) |d_{12}d_{34}\rangle, \tag{34}$$

$$|d_{12}d_{34}\rangle = ((1, 2)_1, (3, 4)_1)_S [[1, 2]_0, [3, 4]_0]_0 \frac{1}{\sqrt{2}} (e^{i\mathbf{p} \cdot \mathbf{r}} + (-)^L e^{-i\mathbf{p} \cdot \mathbf{r}}), \tag{35}$$

where $(i, j)_s$ ($[i, j]_T$) are the spin (isospin) Clebsch-Gordan couplings, with magnetic quantum numbers suppressed, for nucleons, or nucleon pairs, i and j coupling to spin s (isospin

T). Here, P_{ij} is the permutation operator of the indicated nucleons. The symmetry requirements for the exchange of the deuterons are represented by the (orbital-angular-momentum dependent) combination of plane waves in Eq. (35), with \mathbf{p} as the deuteron relative momentum. Even though the expression for the α state seems to single out a (12)+(34) configuration, it is indeed fully anti-symmetric in all indices. This particular form is used because it closely matches the form of the initial-state wave functions, simplifying the evaluation of the spin-isospin summations in the matrix element. The dd wave function can in practice be simplified to

$$|dd\rangle = \sqrt{6} ((1, 2)_1, (3, 4)_1)_S [[1, 2]_0, [3, 4]_0]_0 (2L + 1) i^L j_L(pr) P_L(\hat{\mathbf{p}} \cdot \hat{\mathbf{r}}), \quad (36)$$

since each of the three terms in Eq. (34) gives identical contributions to the matrix element, and $e^{i\mathbf{p} \cdot \mathbf{r}} + (-)^L e^{-i\mathbf{p} \cdot \mathbf{r}}$ reduces to $2(2L + 1) i^L j_L(pr) P_L(\hat{\mathbf{p}} \cdot \hat{\mathbf{r}})$ for any particular partial wave.

We may obtain selection rules for the CSB amplitudes that can contribute by comparing this expression for the deuterons with the α -particle wave function. It is clear that matching the first term of $|\alpha\rangle$ involves no nucleon spin or isospin flips, but to match the second term, the spin and isospin of two nucleons (one from each deuteron) need to be flipped simultaneously. Of course, the overall spin has to change in both cases.

In an explicit and straightforward representation, the above spin-isospin wave functions can be written as

$$|\alpha\rangle = \frac{1}{2\sqrt{6}} \left\{ \left[\uparrow\uparrow\downarrow\downarrow + \downarrow\downarrow\uparrow\uparrow - \frac{1}{2}(\uparrow\downarrow\uparrow\downarrow + \downarrow\uparrow\downarrow\uparrow + \uparrow\downarrow\downarrow\uparrow + \downarrow\uparrow\uparrow\downarrow) \right] (pn\bar{p}n + n\bar{p}n\bar{p} - p\bar{n}n\bar{p} - n\bar{n}p\bar{n}) \right. \\ \left. - (\uparrow\downarrow\uparrow\downarrow + \downarrow\uparrow\downarrow\uparrow - \uparrow\downarrow\downarrow\uparrow - \downarrow\uparrow\uparrow\downarrow) \left[p\bar{p}n\bar{n} + n\bar{n}p\bar{p} - \frac{1}{2}(pn\bar{p}n + n\bar{p}n\bar{p} + p\bar{n}n\bar{p} + n\bar{n}p\bar{n}) \right] \right\}, \quad (37)$$

$$|d_{12}d_{34}10\rangle = \frac{\sqrt{6}}{2\sqrt{2}} (\uparrow\uparrow\downarrow\downarrow - \downarrow\downarrow\uparrow\uparrow) (pn\bar{p}n + n\bar{p}n\bar{p} - p\bar{n}n\bar{p} - n\bar{n}p\bar{n}) 3i j_1(pr) P_1(\hat{\mathbf{p}} \cdot \hat{\mathbf{r}}), \quad (38)$$

where the arrows indicate spin projections and p/n proton and neutron isospin states. Note that for the dd state, only the spin-1, $m_S = 0$ state is given. These expressions can then be used together with the Pauli matrices of the pion production amplitudes to find the formulas for the matrix elements.

In the normalization used here, the spin-averaged cross section (for s -wave pions) is given by

$$\sigma = \frac{1}{16\pi s} \frac{p_\pi}{p} \frac{1}{9} \sum_{\text{pol.}} |\mathcal{M}|^2, \quad (39)$$

where the summation is over the deuteron polarizations.

The CSB operators can now be evaluated in this model and studied in more detail. We will start with the simplest operator (i.e., the one-body term) and use its matrix element as a reference point for the values of the other amplitudes.

A. One-body operator

The one-body amplitude is strongly favored by the symmetries of initial and final states because all of the nucleons contribute coherently to the cross section. However, it does not provide momentum sharing between the deuterons and is hence dependent on the shape of the high-momentum tail of the α -particle wave function. The matrix element for this operator is

$$\mathcal{M}_1 = -i\frac{\Lambda_1}{2}\mathbf{p} \cdot (\boldsymbol{\epsilon}_1 \times \boldsymbol{\epsilon}_2)4\mathcal{W}_1, \quad (40)$$

$$\mathcal{W}_1 = \sqrt{2E_\alpha s} \int d^3r d^3\rho_1 d^3\rho_2 \Psi_\alpha^*(pr) \Phi_1 \Phi_2, \quad (41)$$

where $\boldsymbol{\epsilon}_1$ and $\boldsymbol{\epsilon}_2$ are the polarization vectors of the initial deuterons and the factor of 4 arises from the sum over all nucleons. Thus the spin-momentum structure of the 3P_0s partial wave has been separated from the dimensionless form factor \mathcal{W}_1 . For Gaussian wave functions this matrix element and the corresponding cross section can be calculated analytically. They are

$$\mathcal{M}_1 = -i\frac{\Lambda_1}{2}4\mathbf{p} \cdot (\boldsymbol{\epsilon}_1 \times \boldsymbol{\epsilon}_2) \frac{32\pi^{3/4}\sqrt{E_\alpha s}\alpha^{9/2}\beta^3}{(\alpha^2 + 2\beta^2)^3} \exp\left(-\frac{\alpha^2 p^2}{8}\right), \quad (42)$$

$$\sigma_1 = \frac{512\sqrt{\pi}}{9}\Lambda_1^2 p_\pi p \frac{E_\alpha \alpha^9 \beta^6}{(\alpha^2 + 2\beta^2)^6} \exp\left(-\frac{\alpha^2 p^2}{4}\right), \quad (43)$$

where the exponential stems from the Fourier transform of the α -particle wave function and reflects the dependence on its high-momentum tail. We will use this one-body estimate as the benchmark for the calculations of more complicated amplitudes, and also for the full calculation using realistic wave functions.

B. Meson-exchange operators

Although the seagull amplitude is leading order in χ PT, it is suppressed in our plane wave treatment of the $dd \rightarrow \alpha\pi^0$ reaction because of the combination of two τ matrices

and one σ matrix, which gives a poor match of the initial and final states in our simplified model. Thus, the pion exchange is allowed only between nucleons from the same deuteron, forbidding an advantageous momentum sharing between the deuterons. In addition, the \mathbf{q}_i term vanishes, leaving the recoil term $(\omega/M)\mathbf{k}_i$ as the only contribution. This term is NNLO. The pion-exchange matrix element is

$$\mathcal{M}_\pi = -i\frac{\Lambda_1}{2}\mathbf{p} \cdot (\boldsymbol{\epsilon}_1 \times \boldsymbol{\epsilon}_2)4\mathcal{W}_\pi, \quad (44)$$

$$\mathcal{W}_\pi = \mathcal{W}_1 \frac{\Lambda_\pi}{\Lambda_1} \langle f_{12}^\pi \rangle, \quad (45)$$

$$\Lambda_\pi = \frac{\left(\delta M - \frac{1}{2}\bar{\delta}M\right)\omega}{f_\pi^2} \frac{M}{M}, \quad (46)$$

$$\langle f_{12}^\pi \rangle = \frac{1}{\mathcal{W}_1} \sqrt{2E_\alpha s} \int d^3r d^3\rho_1 d^3\rho_2 \Psi_\alpha^* f_{12}^\pi j_0(pr) \Phi_1 \Phi_2. \quad (47)$$

The matrix element for σ -meson exchange is

$$\mathcal{M}_\sigma = -i\frac{\Lambda_1}{2}\mathbf{p} \cdot (\boldsymbol{\epsilon}_1 \times \boldsymbol{\epsilon}_2)4\mathcal{W}_\sigma, \quad (48)$$

$$\mathcal{W}_\sigma = \frac{\sqrt{2E_\alpha s}}{p} \frac{1}{4} \int d^3r d^3\rho_1 d^3\rho_2 \Psi_\alpha^* \frac{1}{2} \sum_{i \neq j} \left(-\overleftarrow{\nabla}_i f_{ij}^\sigma + f_{ij}^\sigma \overrightarrow{\nabla}_i \right) 3j_1(pr) \hat{\mathbf{p}} \cdot \hat{\mathbf{r}} \Phi_1 \Phi_2 \quad (49)$$

$$= \mathcal{W}_1 \left(\langle f_{12}^\sigma \rangle + \langle f_{13}^\sigma \rangle + \langle f_{13}'^\sigma \rangle \right), \quad (50)$$

where $f_{ij}j_0(pr)$ has been replaced by $\frac{1}{2p}(-\overleftarrow{\nabla}_i f_{ij} + f_{ij} \overrightarrow{\nabla}_i)j_1(pr)$ because of the symmetrization in Eq. (12). The $\langle f_{ij}^x \rangle$ are defined as the averages

$$\begin{aligned} \langle f_{12}^x \rangle &= \frac{1}{\mathcal{W}_1} \sqrt{2E_\alpha s} \int d^3r d^3\rho_1 d^3\rho_2 \Psi_\alpha^* f_{12}^x j_0(pr) \Phi_1 \Phi_2, \\ \langle f_{13}^x \rangle &= \frac{1}{\mathcal{W}_1} \frac{\sqrt{2E_\alpha s}}{p} \hat{\mathbf{p}} \cdot \int d^3r d^3\rho_1 d^3\rho_2 \Psi_\alpha^* f_{13}^x (\overrightarrow{\nabla}_r + \overrightarrow{\nabla}_{\rho_1} - \overrightarrow{\nabla}_{\rho_2}) 3j_1(pr) \hat{\mathbf{p}} \cdot \hat{\mathbf{r}} \Phi_1 \Phi_2, \\ \langle f_{13}'^x \rangle &= \frac{1}{\mathcal{W}_1} \frac{\sqrt{2E_\alpha s}}{p} \hat{\mathbf{p}} \cdot \int d^3r d^3\rho_1 d^3\rho_2 \Psi_\alpha^* \left(-\overleftarrow{\nabla}_r - \overleftarrow{\nabla}_{\rho_1} + \overleftarrow{\nabla}_{\rho_2} \right) f_{13}^x 3j_1(pr) \hat{\mathbf{p}} \cdot \hat{\mathbf{r}} \Phi_1 \Phi_2, \end{aligned} \quad (51)$$

where x could be any of the heavy mesons. This separates the in-deuteron exchanges f_{12} from exchanges between nucleons from different deuterons (f_{13} and f'_{13}). Exchanges between other pairs of nucleons can be reduced to these two because of the symmetries of the dd and α wave functions. Some of the necessary integrals are presented in the Appendix.

The ω -exchange form factor is given by

$$\mathcal{W}_\omega = \mathcal{W}_1 (-\langle f_{12}^\omega \rangle + 2\langle f_{13}^\omega \rangle), \quad (52)$$

with the same external spin factors as in Eq. (48) and with averages defined as in Eq. (51). Due to cancellations, the $\langle f_{13}^{\omega'} \rangle$ term cannot contribute.

The ρ -exchange amplitude has an isospin factor $\boldsymbol{\tau}_i \cdot \boldsymbol{\tau}_j$ that makes it possible to match the initial-state deuterons with the second term of the α -particle wave function [Eq. (33)], giving sizable exchanges between the deuterons. The large ratio of the ρ tensor to vector couplings enhances this amplitude despite the small value of the ρ coupling constant. The ρ form factor is

$$\mathcal{W}_\rho = \mathcal{W}_1 3 \left[\langle f_{12}^\rho \rangle + (1 + C_\rho) (\langle f_{13}^\rho \rangle - \langle f_{13}^{\rho'} \rangle) \right]. \quad (53)$$

Similarly, the $\rho\omega$ -mixing amplitude has a $\tau_i^3 \tau_j^3$ term that involves the large ρ tensor coupling, which gives a large contribution to CSB for $dd \rightarrow \alpha\pi^0$ and possibly also for $np \rightarrow d\pi^0$. The form factor for $dd \rightarrow \alpha\pi^0$ is

$$\mathcal{W}_{\rho-\omega} = \mathcal{W}_1 \frac{\Lambda_{\rho-\omega}}{\Lambda_1} [(3 + C_\rho) \langle f_{13}^{\rho\omega} \rangle - (1 + C_\rho) \langle f_{13}^{\rho\omega'} \rangle], \quad (54)$$

which follows immediately from the expressions for the ρ and ω exchanges. The f_{12} term vanishes since the $1 + \tau_1^3 \tau_2^3$ term of Eq. (21) gives zero when acting on a deuteron and the $\boldsymbol{\sigma}_1 \times \boldsymbol{\sigma}_2$ term vanishes due to the spin-couplings in the wave functions.

The photon exchange contribution is

$$\mathcal{W}_\gamma = \mathcal{W}_1 \frac{\Lambda_\gamma}{\Lambda_1} [(3 + 2\lambda_p) \langle f_{13}^\gamma \rangle - (1 + 2\lambda_p) \langle f_{13}^{\gamma'} \rangle], \quad (55)$$

where again the f_{12} term vanishes. In the simplified model the photon exchange only occurs between pairs of protons, thus not benefiting from the coherence the other amplitudes experience. However, the relatively large coupling makes this amplitude important.

Thus all HMECs have contributions to $dd \rightarrow \alpha\pi^0$. While there are some cancellations of the in-deuteron (f_{12}) and the derivative (f'_{13}) exchange terms between the different heavy mesons, all the f_{13} contributions are of the same sign. Since in all cases $\langle f_{13} \rangle$ is much larger than $\langle f_{12} \rangle$ and $\langle f'_{13} \rangle$ (see Table II below), they dominate the matrix element and the cross section, adding coherently with each other and also with the one-body and pion-exchange terms. Also the photon graph is of the same sign. Thus the internal spin-isospin symmetries of the $dd:\alpha$ system used here strongly favor the one-body and meson-exchange amplitudes if the plane wave approximation is used. This will be demonstrated quantitatively in Sec. IV.

TABLE II: The Yukawa averages (see text for definitions) evaluated for $dd \rightarrow \alpha\pi^0$ at the two IUCF energies, using Gaussian wave functions.

Operator	$T_d = 228.5$ MeV			$T_d = 231.8$ MeV		
	$\langle f_{12} \rangle$	$\langle f_{13} \rangle$	$\langle f'_{13} \rangle$	$\langle f_{12} \rangle$	$\langle f_{13} \rangle$	$\langle f'_{13} \rangle$
π	0.0172	0	0	0.0172	0	0
σ	0.0292	0.470	0.0220	0.0292	0.490	0.0229
ω	0.0228	0.395	0.0106	0.0228	0.412	0.0111
ρ	0.00095	0.0165	0.00046	0.00095	0.0172	0.00048
$\rho\omega$	0.00445	0.0704	0.00377	0.00445	0.0734	0.00393
γ	0.00073	0.0032	0.00109	0.00073	0.0033	0.00111

IV. RESULTS

The matrix elements of the previous section are evaluated numerically using the simplified (Gaussian) wave functions. At most a double integration with a separate single integral was needed, which was carried out using standard Gauss-Legendre techniques. Explicit formulas for the integrals are presented in the Appendix.

The Yukawa averages are tabulated in Table II for each operator and both energies relevant to the IUCF experiment. The $\langle f_{12} \rangle$ contributions are the same at both energies since the in-deuteron exchange is independent of the energy in our plane-wave model. For completeness the $\langle f_{12} \rangle$ values for $\rho\omega$ and photon exchanges are given, even though these, as discussed above, do not contribute to the matrix element in our simplified model. Note that even though the ρ -exchange, $\rho\omega$ -mixing, and photon integrals are much smaller than those for the other meson exchanges, they will be multiplied by large constant factors in the definitions of the matrix elements, Eqs. (53)–(55). This drastically increases their relative importance.

The matrix elements and cross sections calculated from these averages are given in Table III, individually for each amplitude and as a grand total. For comparison purposes, the experimental cross sections are included and the matrix elements are given relative to the one-body matrix element. All the heavy meson exchanges are of the same order as the one-body term, with the $\rho\omega$ mixing being the largest. Adding all amplitudes gives a total

TABLE III: Matrix elements and cross sections evaluated for $dd \rightarrow \alpha\pi^0$ at the two IUCF energies. The matrix elements are given relative to the one-body matrix element, with the relevant CSB mechanism indicated. The experimental cross sections are also given.

Operator (CSB mech.)	$\mathcal{M}(228.5)$	$\mathcal{M}(231.8)$	$\sigma(228.5)$	$\sigma(231.8)$
	$[\mathcal{M}_1]$	$[\mathcal{M}_1]$	[pb]	[pb]
π ($\delta M, \bar{\delta}M$)	0.128	0.128	0.011	0.014
1 ($\pi\text{-}\eta$)	1	1	0.688	0.869
σ ($\pi\text{-}\eta$)	0.522	0.543	0.187	0.256
ω ($\pi\text{-}\eta$)	0.766	0.801	0.404	0.557
ρ ($\pi\text{-}\eta$)	0.344	0.359	0.082	0.112
$\rho\text{-}\omega$ ($\rho\text{-}\omega$)	1.546	1.612	1.645	2.256
γ (el.-mag.)	1.469	1.517	1.486	1.999
total	5.78	5.96	23.0	30.8
Exp. [17]	—	—	12.7 ± 2.2	15.1 ± 3.1

matrix element that is almost six times that of the one-body, increasing the cross section from a meager 0.69 pb at $T_d = 228.5$ MeV (0.87 pb at 231.8 MeV) to 23 pb (31 pb). This is of the same order as the IUCF data $\sigma = 12.7 \pm 2.2$ pb and 15.1 ± 3.1 pb. Note that the cross section is not strictly linear in the pion momentum — the momentum transfer in the wave functions introduces a dependence on the deuteron momentum, which modifies the linearity, at least in this simplified model. For example, Eq. (43) for the one body term contains the square of the deuteron momentum in an exponential.

The relative proportions of the pion-exchange ($\delta M - \frac{1}{2}\bar{\delta}M$), photon exchange, $\rho\text{-}\omega$ -, and $\pi\text{-}\eta$ -mixing (sum of one-body and HMEC) contributions to the matrix element are roughly $\pi\text{:}\gamma\text{:}\rho\text{-}\omega\text{:}\pi\text{-}\eta = 1:11:12:21$. Thus the formally leading seagull terms make up only about 2% of the total matrix element. The total cross section can be expressed in terms of the relative contributions of the different CSB mechanisms such that the dependences on the corresponding parameters are made explicit:

$$\sigma(228.5 \text{ MeV}) = (23.0 \text{ pb}) \left(0.254 + 0.0188 \frac{\delta M}{2.03 \text{ MeV}} + 0.0034 \frac{\bar{\delta}M}{-0.74 \text{ MeV}} \right)$$

$$+ 0.456 \frac{g_{\eta NN}}{\sqrt{4\pi \cdot 0.51}} \frac{\langle \eta | H | \pi^0 \rangle}{(-4200 \text{ MeV}^2)} + 0.268 \frac{g_\rho g_\omega}{4\pi \sqrt{0.43 \cdot 10.6}} \frac{\langle \omega | H | \rho^0 \rangle}{(-4300 \text{ MeV}^2)} \Big)^2. \quad (56)$$

Here the numerical coefficients are the fractions of the matrix element belonging to each of the considered mechanisms, assuming our choice of parameter values. The various terms are normalized, as indicated, to these values. The photon exchange diagram is represented by just a number, since its parameters are well-known. Note that the second and third terms are constrained by the neutron-proton mass difference [Eq. (3)]. The η - π^0 -mixing term can be further separated to show the relative contribution of the various HMEs. Thus,

$$\sqrt{\sigma_{\pi\eta}} = \left(2.18 \sqrt{\text{pb}} \right) \left(0.380 + 0.198 \frac{g_\sigma^2}{4\pi \cdot 7.1} + 0.291 \frac{g_\omega^2}{4\pi \cdot 10.6} + 0.131 \frac{g_\rho^2}{4\pi \cdot 0.43} \right), \quad (57)$$

where $\sigma_{\pi\eta}$ is the cross section from π - η contributions alone and the first number in the second parenthesis is the one-body contribution. At the higher IUCF energy the relative weights of the different contributions in Eqs. (56) and (57) remain more or less the same, with only minor changes. The sensitivity of the cross section calculation to a different choice of couplings can easily be found from these two formulas. For example, using instead the large $g_\eta^2/4\pi = 3.68$ and $\langle \eta | H | \pi^0 \rangle = -5900 \text{ MeV}^2$ as in Ref. [33], the cross section increases from 23 to 118 pb (31 to 158 pb at 231.8 MeV).

V. DISCUSSION

Our simplified model keeps a complete treatment of the dominant pieces of the spin-isospin couplings in the bound state wave functions, even though it ignores some dynamics of the $dd \rightarrow \alpha\pi^0$ reaction and the distortion of the initial state. As a result, the symmetries of the bound state wave functions allow us to determine the CSB amplitudes that are guaranteed to be important for a full calculation.

This treatment shows that the LO π -rescattering term (from the the seagull interactions) is suppressed because of a poor overlap with the initial- and final-state wave functions. Photon loops, at NLO, vanish due to symmetries and cancellations, while a three-body contribution might survive, but has not yet been calculated. On the other hand, the NNLO one-body amplitude and N⁴LO heavy-meson exchanges are strongly favored, adding coherently with each other. Their dominance would be even more spectacular if a larger value for the ηNN coupling were used. Also the ρ - ω -mixing and photon-exchange terms are important and enter at the same level as the one-body and HMEC terms.

We note that our analysis assumes that pions are produced in *s*-waves, as one would expect for a near-threshold reaction. This is supported by the IUCF experiment, where the energy dependence is consistent with *s*-wave production [17].

If our simple wave functions and the plane wave approximation are used, then, within the resonance saturation picture, the dominant CSB mechanisms for the $dd \rightarrow \alpha\pi^0$ reaction are identified with π - η mixing (one-body enhanced by HMECs), followed by ρ - ω mixing and photon exchange, and finally a small contribution from pion rescattering (related to the neutron-proton mass difference).

The coherent sum of these contributions leads to a cross section of the same order of magnitude as the observed one [17], but more needs to be done before making a detailed assessment of the quality of the agreement between theory and experiment.

It is likely that the relative importance of these amplitudes will be shifted once realistic wave functions are used. Preliminary calculations suggest that the one-body term can in fact be enhanced by as much as a factor of three or four with a realistic α -particle wave function. This is expected, since this amplitude is sensitive to the high-momentum tail of the wave function, which is very small for a Gaussian. Preliminary estimates also show that spin-dependent initial state interactions enhance the pion rescattering contribution. We stress that the HMECs are less sensitive to the α -particle wave function and should remain crucial for the interpretation of CSB in the $dd \rightarrow \alpha\pi^0$ reaction.

A full model calculation, using realistic bound-state and dd -scattering wave functions is needed in order to have a clear understanding of the CSB mechanisms behind the $dd \rightarrow \alpha\pi^0$ reaction. Furthermore, the effects of CSB in the wave functions and some diagrams ignored here, such as the long-range part of the various NNLO pion loops and the N³LO recoil part of the Δ -excitation term, should be included. In particular, it is necessary to include the non-z-graph part of photon exchange, e.g., the Coulomb interaction in the initial and final states (Fig. 3). Such an investigation is currently in progress and will be reported later. The general conclusions and insights from the present paper provide important guidelines for that work.

We note a very interesting parallel between the $dd \rightarrow \alpha\pi^0$ process considered here, and the reaction $pp \rightarrow pp\pi^0$. In both cases, a formally-leading diagram is suppressed and the sub-leading diagrams are crucial to explain the cross section. Despite several serious efforts that have yielded substantial insights into the various $NN \rightarrow NN\pi$ systems, the $pp \rightarrow pp\pi^0$

reaction is still not completely understood, especially regarding spin observables [50].

Higher-order interactions — such as the heavy-meson-exchange terms, which could increase the role of π - η mixing — might help improve the agreement between the TRIUMF result for $A_{\text{fb}}(np \rightarrow d\pi^0)$ [16] and theoretical estimates based on reasonable values for δM and $\bar{\delta}M$ [33]. It is thus necessary that a future calculation of $A_{\text{fb}}(np \rightarrow d\pi^0)$ includes these higher-order terms. The three reactions $pp \rightarrow pp\pi^0$, $np \rightarrow d\pi^0$, and $dd \rightarrow \alpha\pi^0$ provide important testing grounds for any pion-production model that intends to include effects beyond-leading-order.

Acknowledgments

We are grateful to Andrew Bacher, Edward Stephenson and Allena Opper for encouragement, many useful discussions, and providing results from the IUCF and TRIUMF experiments prior to publication. We thank Ulf-G. Meißner for useful discussions. We are grateful to the National Institute for Nuclear Theory at the University of Washington for its hospitality and for arranging CSB workshops where part of this work was completed. U.v.K. is grateful to the Nuclear Theory Group at the University of Washington for its hospitality, and to RIKEN, Brookhaven National Laboratory and the U.S. Department of Energy [DE-AC02-98CH10886] for providing the facilities essential for the completion of this work. G.A.M. thanks the ECT* (Trento), the INT (UW, Seattle), and the CSSM (Adelaide) for providing hospitality during the completion of this work. This work was supported in part by the Magnus Ehrnrooth Foundation (J.A.N.), the grant POCTI/FNU/37280/2001 (A.C.F), the NSF grant NSF-PHY-00-70368 (A.G.), the DOE grants DE-FG02-87ER40365 (C.J.H.), DE-FG02-93ER40756 and DE-FG02-02ER41218 (A.G.), DE-FC02-01ER41187 and DE-FG03-00ER41132 (A.N.), DE-FG-02-97ER41014 (G.A.M.), and DE-FG03-01ER41196 (U.v.K.), and by an Alfred P. Sloan Fellowship (U.v.K.).

APPENDIX: EXPLICIT EXPRESSIONS FOR YUKAWA AVERAGES

The averages of the different Yukawa factors of Eq. (51) can be reduced to at most two-dimensional integrals, using the Gaussian wave functions of Sec. III. The angular and one

of the radial integrals can be carried out analytically, resulting in the explicit formulas

$$\begin{aligned}
\langle f_{12}^x \rangle &= \frac{1}{\mathcal{F}_1} \int d\rho_1 \rho_1^2 f_{12}^x e^{-\frac{\rho_1^2}{\gamma^2}} \int d\rho_2 \rho_2^2 e^{-\frac{\rho_2^2}{\gamma^2}} p \int dr r^2 j_0(pr) e^{-\frac{2r^2}{\alpha^2}}, \\
\langle f_{13}^x \rangle &= \frac{1}{\mathcal{F}_1} \int d\rho \rho^2 e^{-\frac{2\rho^2}{\gamma^2}} \left\{ p \gamma^2 \int dr r j_0(pr) e^{-\frac{2r^2}{\alpha^2}} \int dr_{13} r_{13} f_{13}^x \left(e^{-\frac{2(r_{13}-r)^2}{\gamma^2}} - e^{-\frac{2(r_{13}+r)^2}{\gamma^2}} \right) \right. \\
&\quad \left. - \frac{2\gamma^2}{\beta^2} \int dr j_1(pr) e^{-\frac{2r^2}{\alpha^2}} dr_{13} r_{13} f_{13}^x \right. \\
&\quad \times \left. \left[\left(rr_{13} - \frac{\gamma^2}{4} - r^2 \right) e^{-\frac{2(r_{13}-r)^2}{\gamma^2}} + \left(rr_{13} + \frac{\gamma^2}{4} + r^2 \right) e^{-\frac{2(r_{13}+r)^2}{\gamma^2}} \right] \right\}, \\
\langle f'_{13}^x \rangle &= \frac{1}{\mathcal{F}_1} \frac{4\gamma^2}{\alpha^2} \int d\rho \rho^2 e^{-\frac{2\rho^2}{\gamma^2}} \int dr j_1(pr) e^{-\frac{2r^2}{\alpha^2}} dr_{13} r_{13} f_{13}^x \\
&\quad \times \left[\left(rr_{13} - \frac{\gamma^2}{4} \right) e^{-\frac{2(r_{13}-r)^2}{\gamma^2}} + \left(rr_{13} + \frac{\gamma^2}{4} \right) e^{-\frac{2(r_{13}+r)^2}{\gamma^2}} \right], \\
\mathcal{F}_1 &= \left[\int d\rho \rho^2 e^{-\frac{\rho^2}{\gamma^2}} \right]^2 p \int dr r^2 j_0(pr) e^{-\frac{2r^2}{\alpha^2}}, \tag{A.1}
\end{aligned}$$

where $r_{13} = |\mathbf{r}_1 - \mathbf{r}_3|$ and $1/\gamma^2 = 1/\alpha^2 + 1/(2\beta^2)$.

[1] G. A. Miller, B. M. K. Nefkens, and I. Šlaus, *Phys. Rep.* **194**, 1 (1990).

[2] S. Weinberg, *Trans. N.Y. Acad. Sci.* **38**, 185 (1977).

[3] H. Leutwyler, *Phys. Lett.* **B378**, 313 (1996).

[4] L. M. Barkov *et al.*, *Nucl. Phys. B* **256**, 365 (1985).

[5] J. A. Nolen and J. P. Schiffer, *Ann. Rev. Nucl. Part. Sci.* **19**, 471 (1969).

[6] B. Gabioud *et al.*, *Phys. Rev. Lett.* **42**, 1508 (1979); *Nucl. Phys.* **A420**, 496 (1984).

[7] R. Abegg *et al.*, *Phys. Rev. Lett.* **56**, 2571 (1986); R. Abegg *et al.*, *Phys. Rev. D* **39**, 2464 (1989); S. E. Vigdor *et al.*, *Phys. Rev. C* **46**, 410 (1992); R. Abegg *et al.*, *Phys. Rev. C* **57**, 2126 (1998); G. A. Miller, A. W. Thomas, and A. G. Williams, *Phys. Rev. Lett.* **56**, 2567 (1986); A. G. Williams, A. W. Thomas, and G. A. Miller, *Phys. Rev. C* **36**, 1956 (1987).

[8] N. Fettes and U.-G. Meißner, *Nucl. Phys. A* **693**, 693 (2001); and references therein.

[9] L. I. Lapidus, *Zh. Eksp. Teor. Fiz.* **31**, 865 (1956) [Sov. Phys. JETP **4**, 740 (1957)].

[10] N. E. Booth, O. Chamberlain, and E. H. Rogers, *Bull. Am. Phys. Soc.* **4**, 446 (1959); *Nuovo Cimento* **19**, 853 (1961); Y. K. Akimov, O. V. Savchenko, and L. M. Soroko, *Zh. Eksp. Teor. Fiz.* **41**, 708 (1961) [Sov. Phys. JETP **14**, 512 (1962)]; J. A. Poirier and M. Pripstein, *Phys. Rev.* **122**, 1917 (1961); **130**, 1171 (1963).

- [11] J. Banaigs *et al.*, Phys. Lett. **B53**, 390 (1974); Phys. Rev. Lett. **58**, 1922 (1987).
- [12] L. Goldzahl, J. Banaigs, J. Berger, F. L. Fabbri, J. Hüfner, and L. Satta, Nucl. Phys. **A533**, 675 (1991).
- [13] P. Fleury and F. Plouin, “Status Report LNS Expt. 105”, (1987) (unpublished).
- [14] D. Dobrokhoto, G. Fäldt, A. Gårdestig, and C. Wilkin, Phys. Rev. Lett. **83**, 5246 (1999).
- [15] A. Gårdestig, G. Fäldt, and C. Wilkin, Phys. Rev. C **59**, 2608 (1999).
- [16] A. K. Opper *et al.*, Phys. Rev. Lett. **91**, 212302 (2003).
- [17] E. J. Stephenson *et al.*, Phys. Rev. Lett. **91**, 142302 (2003).
- [18] V. Bernard, N. Kaiser, and U.-G. Meißner, Int. J. Mod. Phys. E **4**, 193 (1995).
- [19] P. F. Bedaque and U. van Kolck, Ann. Rev. Nucl. Part. Sci. **52**, 339 (2002).
- [20] T. D. Cohen, J. L. Friar, G. A. Miller, and U. van Kolck, Phys. Rev. C **53**, 2661 (1996).
- [21] U. van Kolck, G. A. Miller, and D. O. Riska, Phys. Lett. **B388**, 679 (1996).
- [22] C. A. da Rocha, G. A. Miller, and U. van Kolck, Phys. Rev. C **61**, 034613 (2000).
- [23] C. Hanhart, U. van Kolck, and G. A. Miller, Phys. Rev. Lett. **85**, 2905 (2000).
- [24] C. Hanhart and N. Kaiser, Phys. Rev. C **66**, 054005 (2002).
- [25] B. Y. Park, F. Myhrer, J. R. Morones, T. Meißner, and K. Kubodera, Phys. Rev. C **53**, 1519 (1996); T. Sato, T.-S. H. Lee, F. Myhrer, and K. Kubodera, Phys. Rev. C **56**, 1246 (1997); C. Hanhart, J. Haidenbauer, M. Hoffmann, U.-G. Meißner, and J. Speth, Phys. Lett. **B424**, 8 (1998); V. Dmitrasinovic, K. Kubodera, F. Myhrer, and T. Sato, Phys. Lett. **B465**, 43 (1999); E. Gedalin, A. Moalem, and L. Razdolskaya, Phys. Rev. C **60**, 031001 (1999); V. Bernard, N. Kaiser, and U.-G. Meißner, Eur. Phys. J. **A4**, 259 (1999); S. Ando, T.-S. Park, and D.-P. Min, Phys. Lett. **B509**, 253 (2001).
- [26] U. van Kolck, Few-Body Syst. Suppl. **9**, 444 (1995); Ph.D. Dissertation, U. of Texas (1993).
- [27] S. Weinberg, in *Chiral Dynamics: Theory and Experiment*, edited by A. M. Bernstein and B. R. Holstein (Springer-Verlag, 1995).
- [28] G. Ecker, J. Gasser, A. Pich, and E. de Rafael, Nucl. Phys. B **321**, 311 (1989).
- [29] E. Epelbaum, U. G. Meißner, W. Glöckle, and C. Elster, Phys. Rev. C **65**, 044001 (2002).
- [30] U. van Kolck, J. L. Friar, and T. Goldman, Phys. Lett. **B371**, 169 (1996).
- [31] C. Y. Cheung, E. M. Henley, and G. A. Miller, Nucl. Phys. A **305**, 342 (1978).
- [32] J. A. Niskanen, Few-Body Syst. **26**, 241 (1999).
- [33] U. van Kolck, J. A. Niskanen, and G. A. Miller, Phys. Lett. **B493**, 65 (2000).

[34] S. A. Coon and B. M. Freedman, Phys. Rev. C **33**, 605 (1986); see also a calculation applicable to the energy region of the (3,3) resonance: C. Y. Cheung, Phys. Lett. **B119**, 47 (1982).

[35] J. Gasser and H. Leutwyler, Phys. Rep. **87**, 77 (1982).

[36] V. G. J. Stoks, R. A. M. Klomp, M. C. M. Rentmeester, and J. J. de Swart, Phys. Rev. C **48**, 792 (1993); U. van Kolck, M. C. M. Rentmeester, J. L. Friar, T. Goldman, and J. J. de Swart, Phys. Rev. Lett. **80**, 4386 (1998).

[37] E. Epelbaum, A. Nogga, W. Glöckle, H. Kamada, U.-G. Meißner, and H. Witała, Phys. Rev. C **66**, 064001 (2002); Eur. Phys. J. **A15**, 543 (2002).

[38] All OBE parameters are adapted from T. E. O. Ericson and W. Weise, *Pions and Nuclei*, (Oxford University Press, New York, 1988).

[39] C. Hanhart, G. A. Miller, F. Myhrer, T. Sato, and U. van Kolck, Phys. Rev. C **63**, 044002 (2001).

[40] S. A. Coon and M. D. Scadron, Phys. Rev. C **51**, 2923 (1995).

[41] L. Tiator *et al.*, Nucl. Phys. **A580**, 455 (1994).

[42] O. Dumbrajs *et al.*, Nucl. Phys. **B216**, 277 (1983).

[43] R. Machleidt, C. Elster, and K. Holinde, Phys. Rep. **149**, 1 (1987); R. Machleidt, Adv. Nucl. Phys. **19**, 189 (1989).

[44] R. Machleidt, Phys. Rev. C **63**, 024001 (2001).

[45] R. P. Springer, Phys. Lett. **B461**, 167 (1999).

[46] T.-S. H. Lee and D. O. Riska, Phys. Rev. Lett. **70**, 2237 (1993).

[47] C. J. Horowitz, H. O. Meyer, and D. K. Griegel, Phys. Rev. C **49**, 1337 (1994).

[48] S. Gardner and H. B. O'Connell, Phys. Rev. D **57**, 2716 (1998); **62**, 019903(E) (2000).

[49] J. Carlson and R. Schiavilla, Rev. Mod. Phys. **70**, 743 (1998).

[50] H. O. Meyer *et al.*, Phys. Rev. C **63**, 064002 (2001); C. Hanhart, hep-ph/0311341.

[51] This assignment has no deeper reason than the numerical proximity of $\sqrt{m_\pi M} = 2.6m_\pi$ and $M_\Delta - M = 2.1m_\pi$.

[52] Apart from the pion mass itself, the effects of explicit chiral symmetry breaking are typically sub-leading. As a consequence, quark-mass isospin breaking is in general smaller than it would be expected on the basis of the quark mass splitting, $\epsilon \sim 1/3$ [26].

[53] Note that the leading $\gamma\pi NN$ vertex — the so-called Kroll-Rudermann term — couples to the pion charge and therefore does not directly contribute to neutral-pion production.